BANCA D'ITALIA
EUROSISTEMA

Temi di discussione

(Working Papers)

Volatility bursts: a discrete-time option model with multiple volatility components

by Francesca Lilla

June 2021

Number 1336

BANCA D'ITALIA
EUROSISTEMA

Temi di discussione

(Working Papers)

Volatility bursts: a discrete-time option model with multiple volatility components

by Francesca Lilla

Number 1336 - June 2021

ISSN 1594-7939 (print)
ISSN 2281-3950 (online)

Printed by the Printing and Publishing Division of the Bank of Italy

VOLATILITY BURSTS: A DISCRETE-TIME OPTION MODEL WITH MULTIPLE VOLATILITY COMPONENTS

by Francesca Lilla*

Abstract

I propose an affine discrete-time model, called Vector Autoregressive Gamma with volatility Bursts (VARG-B), in which volatility, in addition to frequent and small changes is characterized by periods of sudden and extreme movements generated by a latent factor, which evolves according to the Autoregressive Gamma Zero process. One key advantage of the discrete-time specification is that it makes it possible to estimate the model via the Extended Kalman Filter. Moreover, the VARG-B model leads to a fully analytic conditional Laplace transform, resulting in a closed-form option pricing formula. When estimated on S&P500 index options and returns, the new model provides more accurate option pricing and modelling of the IV surface compared with a number of alternative models.

JEL Classification: C13, G12, G13.
Keywords: volatility bursts, ARG-zero, option pricing, Kalman filter, realized volatility.
DOI: 10.32057/0.TD.2021.1336

Contents

* Bank of Italy, Directorate General for Economics, Statistics and Research - Statistical Analysis.

1 Introduction[1]

The price of options depends on ”extreme” movements of the underlying asset price, in addition to idiosyncratic asset changes. Since asset prices must follow semimartingales to avoid arbitrage opportunities, the literature has mainly focused on continuous time models. In this framework, extreme movements (typically associated with unexpected macroeconomic news announcements) are commonly modelled as discontinuities in the price trajectories: jumps. Starting from the seminal paper of Merton (1976), methods to distinguish between volatility and jump risk were assessed to fit low frequency data. However, the results provided in Christensen, Oomen, and Podolskij (2014) (COP henceforth) weaken the consensus in the literature about the presence of jumps in asset price! Using intraday data, COP examine the role of the jump component by applying new econometric techniques to a set of individual order-level tick data. The authors find that jumps account for only about 1% of quadratic price variation, which is substantially smaller than what typically found by lower-frequency literature. Moreover, COP show that the price continuity is often preserved. They suggest that sharp movements of asset prices over short periods of time are generated by high volatility episodes instead of genuine price jumps. The much reduced role for jumps and, consequently, the elevated role for volatility process, calls for a stronger effort in modelling the volatility dynamics and carries important implications for asset pricing models.

One goal of this paper is to replace jumps with volatility bursts in the dynamics of the underlying and understand if this replacement carries over to option valuation! This challenge is addressed in discrete time by specifying an affine discrete-time model, called Vector Autoregressive Gamma with volatility Bursts (VARG-B), which is characterised by a multifactor volatility specification. In the VARG-B model volatility experiences, in addition to frequent and small changes, periods of sudden and extreme movements, i.e.

[1]I would like to thank Sergio Pastorello, Roberto Renó, Fulvio Corsi, Giacomo Bormetti and Cecilia Mancini for their helpful comments and suggestions. The views expressed in this paper are those of the author and do not necessarily reflect those of the Bank of Italy.

volatility bursts. From a modelling perspective, the introduction of volatility bursts in a discrete time setting requires an additional state variable in the volatility dynamics. In this work, the volatility is assumed to be latent, and at each point in time, it is the result of the sum of two independent random variables. The frequent and small changes are generated by the first state variable, called *continuous* component, while the *volatility burst* component generates the volatility changes due to extreme price movements. The first variable is modelled as an Autoregressive Gamma process (ARG), see Gourieroux and Jasiak (2006), while the second follows an Autoregressive Gamma Zero (ARG-Zero) process. This last process is proposed in Monfort et al. (2014) to model the Zero Lower Bound in the term structure of interest rate. The ARG-Zero process, whose introduction into the volatility dynamics represents the main innovation of this paper, is a suitable statistical channel for describing sudden volatility changes since it is coherent with non-negative volatility bursts and it accommodates extended periods of zero or close-to-zero values.

A key advantage of the proposed specification is that the model can be estimated using the Extended Kalman Filter, which allows filtering the time series of both volatility components. Thanks to this flexible estimation strategy it is possible to understand the relative contribution of both the volatility factors to the total conditional variance of log-returns. Moreover, the VARG-B model leads to a fully analytic conditional Laplace transform, thanks to its exponential affine form, which is mainly attractive for option pricing purposes. Indeed, the change of measure is performed adopting an exponentially affine stochastic discount factor which preserves all the analytical results in order to obtain a closed-form option pricing formula. Finally, the affine discrete-time model presented in this paper is intuitive and easy to estimate.

Specifically speaking, the VARG-B model extends the LHARG-RV model by Majewski et al. (2015) in which the volatility does not display sudden, and large changes and is perfectly observed through a realized measure (RM). More recently, Alitab et al. (2020) introduce the jump variation in the volatility dynamics which is, also in this case, observed in all its components through high frequency data-based estimators. To the best of my knowledge Caporin et al. (2015) and Caporin et al. (2017) represent the only attempt at modelling the occurrence and the probability of volatility bursts in a discrete time setting. Caporin et al. (2015) extend the HAR model of Corsi (2009) with a linear and additive volatility burst factor (HAR-V-J, see Andersen et al., 2007 and Corsi et al., 2010) finding a positive probability of volatility bursts which are more likely to happen during financial crises. Caporin et al. (2017) extend the MEM model of Engle and Gallo (2006) with a multiplicative volatility burst factor (MEM-J). The authors find that the MEM-J significantly increases the model fit on the right tail of the volatility distribution[2]. In all these papers the authors assume that the price process is characterised by jumps and except for Alitab et al. (2020) which explicitly provide the jump variation component, they remove the spikes in the RM time series using a local volatility estimator: the RM is assumed to be the proxy of the returns integrated variation. Clearly, assuming the presence of jumps in the price process, the ability to disentangle the two sources of risk, strictly depends on the methodology employed for the jump identification and the results can be driven by the method chosen.

This paper differs from this discrete time literature since the price process is assumed to be free of jumps (following the COP intuition) and the extreme price movements being, instead, a by-product of volatility bursts. Since volatility is assumed to be latent, information about the state variables is recovered through a measurement equation introduced in the estimation procedure.

The empirical results on a large sample of S&P500 Index options emphasise the superior ability of the VARG-B model in pricing options along moneyness and time to maturity dimensions. These findings indicate the benefit of a multi-factor volatility specification that allows for volatility bursts in addition to usual changes.

The paper is organised as follows. In Section 2, I develop the return process and

[2] Caporin et al. (2017) compare alternative MEM specification (no jumps, constant and time-varying jump intensity) with respect to their ability in fitting the dynamics of the series analysing the dynamic properties of the residuals. Moreover, the authors study the ability of the MEM specifications to correctly predict the probability of tail events providing a Volatility-at-Risk exercise.

the volatility dynamics under the historical measure. Section 3 estimates the historical process via pseudo maximum likelihood with Extended Kalman Filter. In Section 4, I propose an economic application where I analyse the performance of the VARG-B model in an option pricing exercise. In particular, I derive the change of measure for the new model. I calibrate the model on options, provide the pricing and analyses its performance. Finally, Section 5 concludes. The proofs of all propositions are provided in the appendix.

2 The VARG-B model

The goal of this section is to build a model for option valuation that allows for volatility bursts in the return dynamics. I develop a model in which volatility is latent in all its components.

2.1 The VARG-B physical dynamics

The VARG-B model explicitly accounts for the probability of having large and sudden movements in the volatility dynamics through an additive component modelled with a new process, i.e. ARG-Zero.

Under the VARG-B specification the discrete-time stochastic volatility model for daily log-returns is the following:

$$y_{t+1} := \log\left(\frac{S_{t+1}}{S_t}\right) = r_{t+1} + \lambda f_{t+1} + \sqrt{f_{t+1}}\epsilon_{t+1} \tag{1}$$

where r_{t+1} denotes the risk-free rate at time $t+1$, assumed to be exogenous, and where λ is the market price of risk. The innovation ϵ_{t+1} is i.i.d. $\mathcal{N}(0,1)$. Moreover, the latent factor f_{t+1} denotes the true volatility, and it is equal to the sum of two independent components:

$$f_{t+1} = f_{1,t+1} + f_{2,t+1}. \tag{2}$$

Given the information set at time t, denoted $\mathcal{F}_t$, the continuous volatility component follows an Autoregressive Gamma (ARG) process:

$$f_{1,t+1}|\mathcal{F}_t \sim \gamma_\nu(\beta_1 f_{1,t}, \mu_1) \quad \textit{for} \quad \nu > 0, \beta_1 > 0, \mu_1 > 0 \tag{3}$$

The process in (3) is defined by a shape parameter ν, a noncentrality parameter $\beta_1 f_{1,t}$ and a scale parameter μ_1. The history of the process determines the entire noncentrality coefficient $\beta_1 f_{1,t}$, which is written as a linear function of the lagged value of the process.

Since the ARG process is a discretized version of the Cox, Ingersoll Jr, and Ross (1985) (CIR) model, it is sufficiently flexible to represent the volatility of financial asset.

Moreover, given $\mathcal{F}_t$ and $f_{1,t+1}$, the volatility burst component follows an Autoregressive Gamma Zero (ARG-Zero) process:

$$f_{2,t+1}|\mathcal{F}_t \sim \gamma_0(d_2 + \beta_2 f_{2,t}, \mu_2) \quad \textit{for} \quad d_2 \geq 0, \beta_2 > 0, \mu_2 > 0 \tag{4}$$

denoted as $ARG_0(d_2 + \beta_2 f_{2,t}, \mu_2)$.

In (2) $f_{1,t+1}$ allows for frequent and small changes that characterize the volatility dynamics and it is called *continuous* volatility component. $f_{2,t+1}$ represents an "exceptional" volatility component that let volatility to experience periods of big and sudden changes. The latter is the focus of this model and is called *volatility burst* component.

On the contrary of the ARG by Gourieroux and Jasiak (2006), the process in (4) is characterised by a zero lower bound: $f_{2,t+1}$ can take zero value with a strictly positive probability, stay at zero for a more or less extended period of time and become positive again. In order to understand the behaviour of an ARG-Zero process, I define its main characteristics.

The conditional probability density function $p(f_{2,t+1}|\mathcal{F}_t)$ of the $ARG_0(d_2 + \beta_2 f_{2,t}, \mu_2)$

is given by:

$$p(f_{2,t+1}|\mathcal{F}_t;\phi) = \sum_{z=1}^{+\infty}\left[\frac{\exp(-f_{2,t+1}/\mu_2)f_{2,t+1}^{z-1}}{(z-1)!\mu_2^z} \times \frac{\exp[-(d_2+\beta_2 f_{2,t})](d_2+\beta_2 f_{2,t})^z}{z!}\right]\mathbb{1}_{\{f_{2,t+1}>0\}} + \exp(-d_2-\beta_2 f_{2,t})\mathbb{1}_{\{f_{2,t+1}=0\}} \tag{5}$$

where $\phi = d_2, \beta_2, \mu_2$.

Moreover, f_{t+1} in (2) is stationary if and only if $\rho_j = \beta_j \mu_j < 1$ for $j = 1, 2$ [3].

The zero-point mass in equation (5) which is allowed by the zero shape parameter emphasizes the key feature of the ARG-Zero process: the zero lower bound. In fact, the probability of $f_{2,t+1}$ of reaching zero is equal to the second term on the right hand side of equation (5), i.e. $\exp(-d_2 - \beta_2 f_{2,t})$. Another important feature of the ARG-Zero process is represented by the positive intercept, i.e. d_2. The conditional probability of $f_{2,t+1}$ of remaining at the zero lower bound is $\exp(-d_2)$. When $d_2 = 0$, the zero lower bound becomes an absorbing state, since $\exp(-d_2) = 1$. On the contrary, the presence of a strictly positive intercept prevents $f_{2,t} = 0$ to be an absorbing state: if $d_2 > 0$, than $\exp(-d_2) < 1$. Indeed, the lower is d_2, the greater is the conditional probability of having more extended periods of zero values for $f_{2,t+1}$.

The VARG-B model in (1)-(4) has an important advantage from the option pricing perspective: it leads to a fully analytic conditional Laplace transform. Despite the complexity of the conditional density function in (5), the conditional Laplace transform is easy to manipulate, and it is equal to:

[3] The stationarity condition for the ARG-Zero process is illustrated in *Corollary 2.1.2* in Monfort et al. (2014). The stationarity condition for the ARG process is shown in *Proposition 2* in Gourieroux and Jasiak (2006).

$$
\begin{aligned}
\varphi_t(u) :&= \mathbb{E}\left[\exp(u_1 f_{1,t+1} + u_2 f_{2,t+1})|\mathcal{F}_t\right] \\
&= \exp\left[\frac{u_1\mu_1}{1-u_1\mu_1}\beta_1 f_{1,t} + \frac{u_2\mu_2}{1-u_2\mu_2}(d_2 + \beta_2 f_{2,t}) - \nu\log(1-u_1\mu_1)\right] \\
&\quad \textit{for} \quad u_1 < \frac{1}{\mu_1} \quad \textit{and} \quad u_2 < \frac{1}{\mu_2}
\end{aligned} \tag{6}
$$

I illustrate the relevance of the ARG-Zero process for volatility bursts modelling with a simple simulation exercise. The dynamics of the volatility burst factor is given by the ARG_0 in (4) with $d_2 = 0.1$ and $\mu_2 = 0.01$.

The chosen parameters are calibrated in such a way that the unconditional mean and the unconditional variance of $f_{2,t}$ are about 0.2 and 0.4, respectively. Given these parameters, I simulate 1000 periods for the process. The conditional probability for $f_{2,t}$ of remaining at zero is equal to $\exp(-d_2) = \exp(-0.1) = 0.9$.

From Figure 1, $f_{2,t}$ is characterised by extreme and sudden changes as well as by many episodes of periods of zero values. This behaviour of the ARG_0 process is particularly appealing to model the extraordinary nature of volatility bursts.

From an economic point of view, if the volatility burst component is modelled as an ARG-Zero process, d_2 identifies the average persistence of zero lower bound regimes. Given the exceptional characteristic of the bursts, d_2 should be greater than zero and small in magnitude. The evidence provided in Section 3.3 confirms this theoretical feature.

3 Model estimation

In the previous section, I have laid out the general framework for incorporating volatility bursts when modelling return dynamics. In this section, I develop a Kalman filter-based estimation method to estimate the physical ($\mathbb{P}$) parameters using daily observations on returns and information about volatility provided by the realized volatility measure (Andersen and Bollerslev, 1998). I also briefly describe two alternative models that I es-

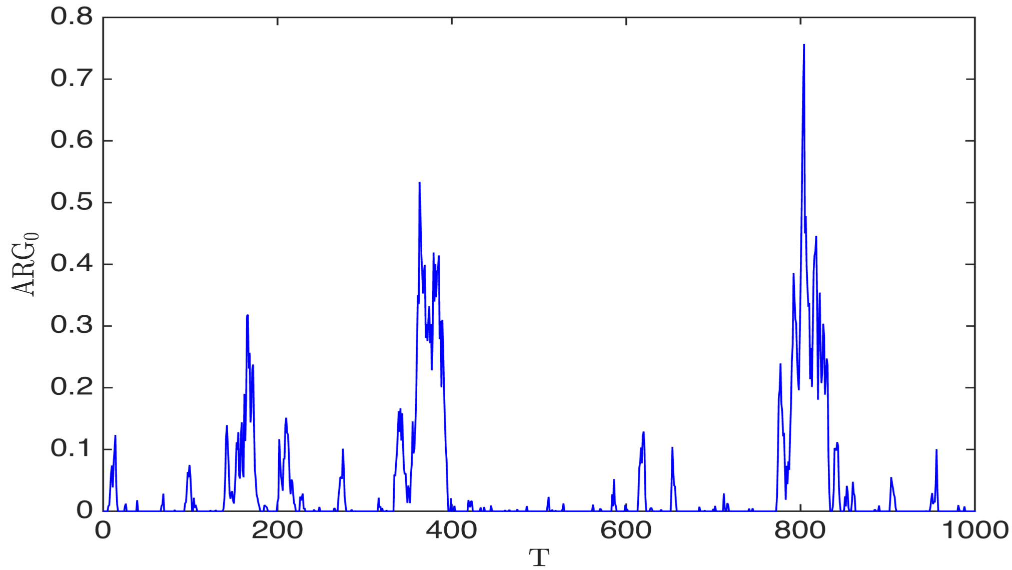

Figure 1: Simulated path of the volatility burst factor defined by the following conditional distribution: $f_{2,t+1}|\mathcal{F}_t \sim \gamma_0(d_2 + \beta_2 f_{2,t}, \nu_2)$. T is the total number of periods considered.

timate in order to have an idea of the relative VARG-B performance. The purpose of this section is dual: to illustrate how to estimate physical parameters on real data, and to propose empirical support to the VARG-B specification in which price jumps are replaced by volatility bursts.

3.1 Estimation strategy

The VARG-B model can be represented in a state-space form which can be estimated via pseudo-maximum likelihood with the Extended Kalman filter. The pseudo maximum likelihood is feasible since the first two conditional moments are available in closed-form. The Kalman filter strategy is natural in this framework since the VARG-B model is affine in the state variables.

The first measurement equation is directly obtained from the daily log-returns dynamics in (1). Assuming that returns of financial assets arise through discrete observations from an underlying continuous-time process, I augment the state space model with a second measurement equation. The latter measurement equation relates the latent volatility to an ex-post estimator of daily quadratic variation of the log-price process over the period $t+1$, i.e. Realized Volatility (RV) by Andersen and Bollerslev (1998).

The transition equations are given by the factor dynamics, specified according to the conditional mean and the conditional variance:

$$E(f_{jt+1}|\mathcal{F}_t) = \mu_j(d_j + \beta_j f_{jt}) + \mu_j \nu_j \qquad \text{for} \quad j = 1,2 \tag{7}$$

$$V(f_{jt+1}|\mathcal{F}_t) = 2\mu_j^2(d_j + \beta_j f_{jt}) + \mu_j^2 \nu_j \qquad \text{for} \quad j = 1,2 \tag{8}$$

where $\nu_1 = \nu$ as defined in (3) and $\nu_2 = 0$ as in (4).

In what follows, I formally lay down the state space model.

Using (7) and (8), the transition equations can be expressed as follows:

$$f_{1,t+1} = \mu_1 \nu + \mu_1 \beta_1 f_{1,t} + \sqrt{\mu_1^2(\nu + 2\beta_1 f_{1,t})} v_{t+1}^1 \tag{9}$$

$$f_{2,t+1} = \mu_2 d_2 + \mu_2 \beta_2 f_{2,t} + \sqrt{\mu_2^2(2d_2 + 2\beta_2 f_{2,t})} v_{t+1}^2 \tag{10}$$

where v_{t+1}^1 and v_{t+1}^2 are independent white noises with zero mean and unit variance.

The measurement equations describe the relationship between two types of observable variables and both the latent volatility factors:

$$y_t = r_t + \lambda(f_{1,t} + f_{2,t}) + \sqrt{f_{1,t} + f_{2,t}} \epsilon_t \tag{11}$$

$$RV_t = \eta_0 + \eta_1(f_{1,t} + f_{2,t}) + \zeta_t \tag{12}$$

$\zeta_t \sim IIDN(0, \sigma^2)$ and ϵ_t and ζ_t are independent.

The innovation term in (12) can be interpreted as a measurement error with zero mean and constant variance. Indeed, the estimator RV is characterised by an attenuation bias generated by the finite nature of the price sample (classic measurement problem) and by the absence of trading during the night (overnight effect).

I estimate parameters in (9)-(12) via pseudo-maximum likelihood with the Extended

Kalman filter. This estimation strategy allows to deal with two problems which makes us depart from the case where the linear Kalman filter is optimal. First, the conditional distribution of the factors in (9) and (10) is not normal but, if the conditional mean and variance of both state variables are correctly specified, I could expect that the estimates obtained from the Kalman filter to be consistent with the QML principle. From a practical point of view this means that the true log-likelihoods derived from conditional non-central Gamma distributions are replaced by Gaussian distributions. Second, the model is nonlinear since the conditional variance of the factors in (9) and (10) depends on the current values of both factors. Since this nonlinearity, the usual Kalman filter cannot be applyied. However, an approximate filter can be obtained by linearizing the model, i.e. applying the Extended Kalman filter. The application of this estimation strategy represents a strength of the VARG-B model. The availability of a state-space model makes the implementation of such a procedure straightforward, letting data dictate the relative contribution of both factors to the total volatility.

3.2 Alternative models

The VARG-B model is a discrete time specification in which the volatility dynamics is given by the sum of two independent factors.

First, by setting $f_{2,t+1} = 0$ in (2), I obtain the standard ARG model by Gourieroux and Jasiak (2006).

Second, I can shut down the volatility burst component, and I can allow for long-memory in volatility, providing the HAR specification of Corsi (2009) for the non-central parameter in (3). In this case, I obtain the HARG model proposed in Corsi et al. (2013). Coherently with the basic idea of Corsi et al. (2013) and Majewski et al. (2015), in both the alternative specifications, the volatility (continuous component only) is assumed to be observed through the RV measure. In this way, the original estimation strategy is maintained and the RV-based option valuation framework is not distorted.

Finally, following the main motivation of this paper, I consider the LHARG-ARJ by

Alitab et al. (2020). The LHARG-ARJ extends the LHARG-RV model by Majewski et al. (2015) by adding a jump component in the log-return dynamics. To guarantee a fair comparison, I dismiss the leverage component from the volatility dynamics and I consider an autoregressive gamma process of order one for the volatility. In this way I can focus on the role of the jump component and the volatility burst factor in generating extreme price movements and, in turn, in pricing options.

3.3 Parameter estimates

The dependent variable in the first measurement equation is defined using daily returns of the S&P500 Index from January 5, 1996 to September 12, 2017. The RV time series in the second measurement equation is obtained using returns on the S&P500 Index from January 5, 1996 to September 12, 2017 sampled at 5 minutes frequency which represents the trade-off between accuracy and microstructure noise (Madhavan, 2000, Biais et al., 2005 and McAleer and Medeiros, 2008 for surveys on this topic).

Based on the two measurement equations (11)-(12) provided in the state space model, daily observations are used to filter both state variables, i.e. continuous and volatility burst. Table 1 shows the estimated parameters, and the relative standard errors for the VARG-B model and the alternative models presented in Section 3.2. According to the estimates, all VARG-B coefficients are statistically different from zero. Note that a significant and small value for the intercept d_2 translates in an increasing ability of the ARG-Zero process to describe extraordinary and exceptional changes in the volatility, thus supporting the proposed specification. On the one hand, a small value for the intercept in (4) increases the probability of having extended periods of zero values after sudden movements. These unexpected changes have a specific persistence given by $\mu_2\beta_2$. On the other hand, a strictly positive value for d_2 prevents the zero lower bound of being an absorbing state. These are the two main features that most motivate a model specification for bursts in the volatility dynamics.

Table 1: Estimate of the parameters under the historical measure and standard errors (in parenthesis) for the VARG-B, ARG, HARG and LHARG-ARJ model. The parameters reported in the first column are estimated via pseudo maximum likelihood with Extended Kalman filter. The parameters of both ARG and HARG models are estimated using Maximum Likelihood. The historical data for all models are daily RV computed on 5-minutes data and daily returns of the S&P500 Index from January 5, 1996 to September 12, 2017.

	VARG-B		ARG		HARG		LHARG-ARJ
Parameter		Parameter		Parameter		Parameter	
λ	-0.0792	λ	1.4350	λ	1.4350	λ_c	1.9000
	0.00002256		1.6132		1.6132		0.000213
ν	0.0195	μ	0.2831	μ	0.2485	λ_j	1.2500
	0.000149		0.0084		0.0077		0.000184
d_2	0.1865	β_d	1.1656	β_d	1.1029	θ	0.2974
	0.0001996		0.01060		0.01059		0.000207
β_2	0.8987	ν	2.3694	β_w	1.6070	k	0.0001
	0.00000068		0.0862		0.2024		
β_1	0.8195			β_m	0.9730	β_d	2.3184
	0.0000418				0.1496		0.00000004
σ	0.0078			ν	0.3480	Λ	-0.0004
	0.0000393				0.1014		0.0000007
η_0	0.2228					δ	0.0023
	0.0000286						0.000191
η_1	0.4380					$\bar{\omega}$	0.0125
	0.0000127						
						ξ	0.7400
							0.000185
						ζ	0.0040
							0.000191
Log-likelihood	-12375		-33286		-32951		-15209

This result is in line with the updated[4] time series of both volatility factors reported in Figure 2. Indeed, $f_{1,t}$ in (3) describes the small and frequent volatility changes while $f_{2,t}$ in (4) allows volatility to experience extraordary movements due to unexpected news. Figure 3 shows the RV and the updated values for $f_t = f_{1,t} + f_{2,t}$. The VARG-B model fits

[4] At each point in time, the current value of the state variable is updated on the basis of the observations of both returns and RV.

volatility changes, measured *ex-post* by RV. As explained before, the measurement error in (12) can be linked to the attenuation bias characterising RV. Indeed, augmenting the state space model with a relation between state variables and observed data deals with the usual errors-in-variables problem.

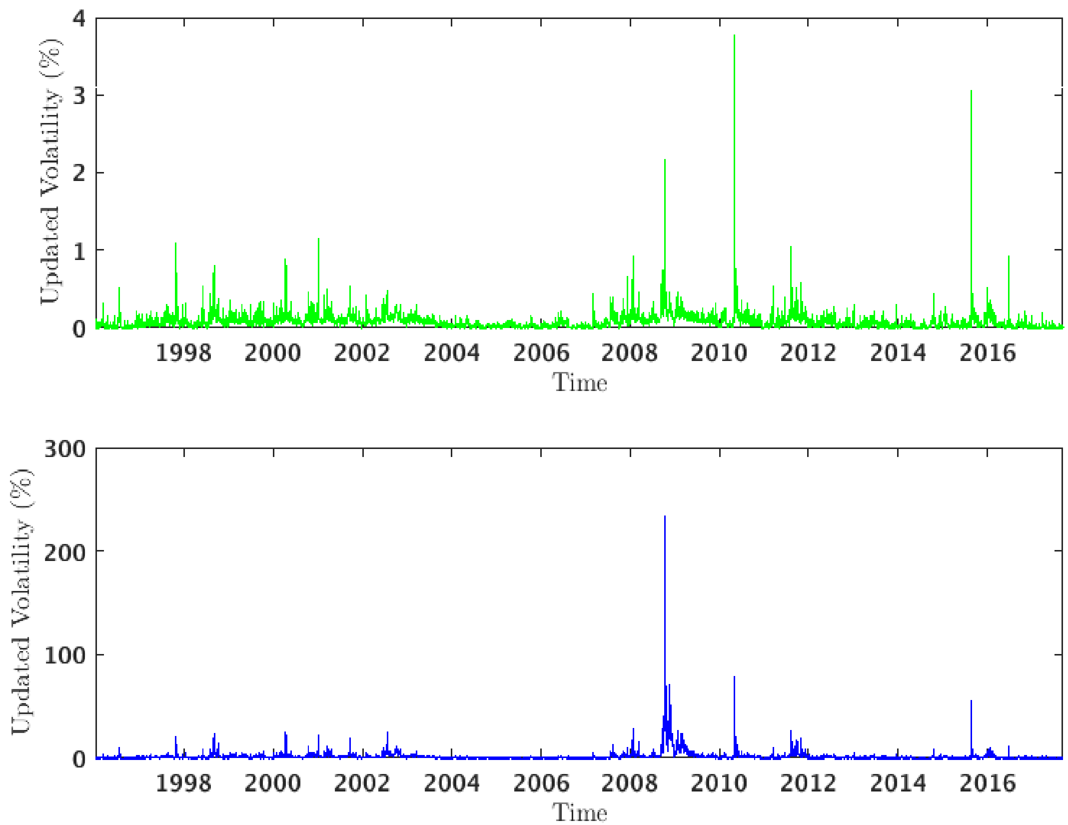

Figure 2: This figure shows the updated time series of the continuous ($f_{1,t}$, green line) and the burst ($f_{2,t}$, blue line) factors which are obtained applying the estimation procedure based on the Kalman filter. The sample consists of S&P500 Index data from January 5, 1996 to September 12, 2017.

The model selection approach based on both the AIC (Akaike, 1998) and the BIC (Schwarz et al., 1978) select the VARG-B to model volatility. In particular, for both information criteria, the VARG-B model registers the smallest value. Indeed among the models presented in this section, the VARG-B offers the best goodness of fit.

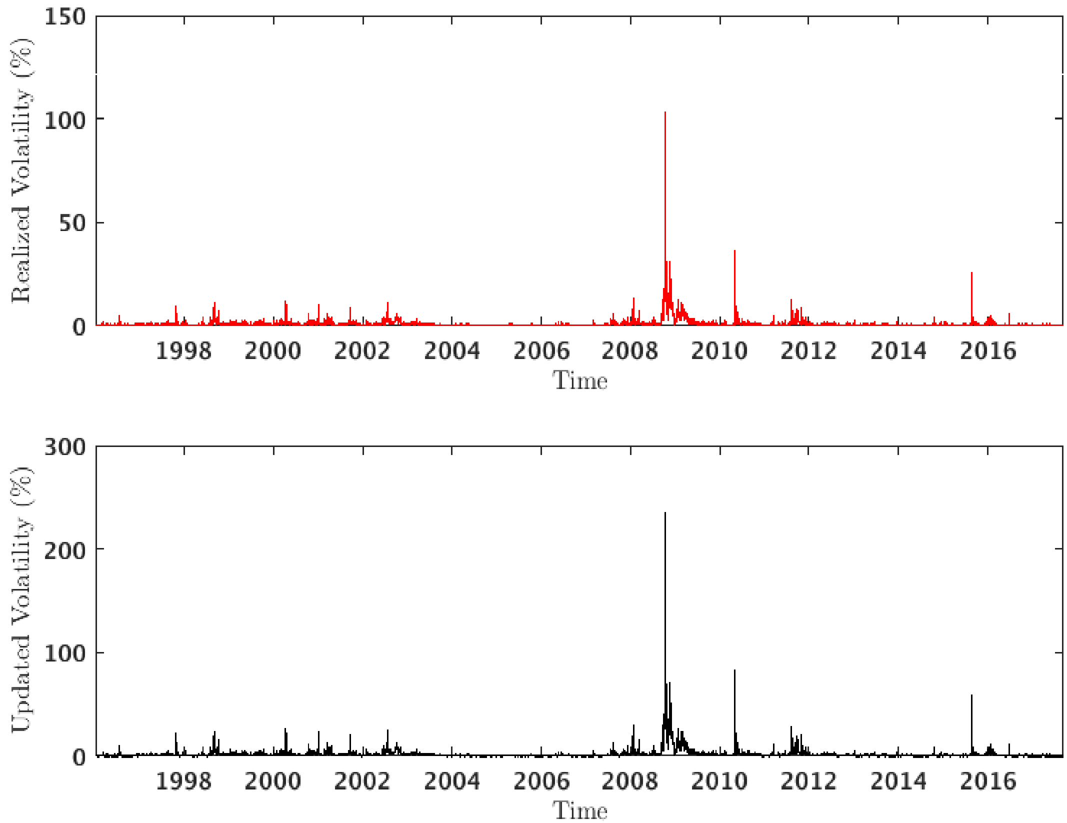

Figure 3: This figure shows the comparison between RV_t (top figure) and the updated time series of f_t (bottom figure). The sample consists of S&P500 Index data from January 5, 1996 to September 12, 2017.

4 Model evaluation

In this section, I show how the VARG-B model developed under the physical measure can be used for option pricing. I first derive the moment generating function under the $\mathbb{P}$ measure for the VARG-B model and show that it is affine. I then define a stochastic discount factor which implies that the risk-neutral ($\mathbb{Q}$) moment generating function is of the same form as its physical counterpart. Then I approximate option prices using the

COS efficient scheme[5] by Fang and Oosterlee (2008). All the propositions presented in this section are directly derived from the theoretical results presented in Majewski et al. (2015). Empirical results and VARG-B pricing performance follow.

4.1 The historical moment generating function

Equations (1) and (3)-(4) completely characterize the VARG-B model under the $\mathbb{P}$ measure. A great advantage of the VARG-B model is that its Moment Generating Function (MGF) satisfies the affine property.

Proposition 1. *The setup in Section 2.1 satisfies the Assumption 1 in Majewski et al. (2015):*

$$\begin{aligned} & \mathbb{E}^{\mathbb{P}}\left[\exp(zy_{t+1} + \mathbf{b}'\mathbf{f}_{t+1})|\mathcal{F}_t\right] \\ = \;& \exp\left[\mathcal{A}(z,\mathbf{b}) + \mathcal{B}(z,\mathbf{b})' \cdot \mathbf{f}_t\right] \end{aligned} \tag{13}$$

for some functions $\mathcal{A} : \mathbb{R} \times \mathbb{R}^k \times \mathbb{R}^k \to \mathbb{R}, \mathcal{B} : \mathbb{R} \times \mathbb{R}^k \times \mathbb{R}^k \to \mathbb{R}^k$ *given in* (A.9) *and* (A.10).

Proof. *See Appendix A.*

Proposition 1 implies that the moment generating function of $\log(S_T/S_t)$ under the $\mathbb{P}$ measure is given by a recursive relation in terms of the functions $\mathcal{A}$ and $\mathcal{B}$.

Proposition 2. *Let* $y_{t,T} = \log(S_T/S_t)$, *under* $\mathbb{P}$, *the MGF for the VARG-B model has the following form*

$$\varphi^{\mathbb{P}}_{t,T,z} = \mathbb{E}^{\mathbb{P}}[e^{zy_{t,T}}|\mathcal{F}_t] = exp\left(a_t + \mathbf{b}_t'\mathbf{f}_t\right) \tag{14}$$

with $z \in \mathbb{R}$, $\mathbf{b} \in \mathbb{R}^2$ *and where*

[5] The COS method is an option pricing numerical method for European options based on the Fourier-cosine series. It takes advantage of the relation of the characteristic function with the series coefficients of the Fourier-cosine expansion of the density function. It is available once the characteristic function of the log-asset price is known and it has been proved to be fast and efficient.

$$
\begin{aligned}
a_s &= a_{s+1} + zr - \nu W_{1,s+1} + d_2 V_{2,s+1} & (15) \\
\mathbf{b}'_s &= \mathbf{b}'_{s+1} + (V_{1,s+1}, V_{2,s+1})\boldsymbol{\beta} & (16)
\end{aligned}
$$

with

$$
x_{h,s+1} = x_h(z, \mathbf{b}_{s+1}) = \mathbf{b}'_{s+1} + z\lambda + \frac{z^2}{2}, \quad h = 1, 2
$$

subject to the initial conditions:

$$
a_T = 0, \quad \mathbf{b}'_T = 0
$$

The functions V and W are defined as follows:

$$
\begin{aligned}
V_{h,s+1} &= V_h(x_{h,s+1}, \mu_h) = \frac{x_{h,s+1}\mu_h}{1 - x_{h,s+1}\mu_h}, \quad h = 1, 2 \\
W_{1,s+1} &= W_1(x_{1,s+1}, \mu_1) = \log\left[1 - x_{1,s+1}\mu_1\right]
\end{aligned}
$$

Proof. *See Appendix D*

The parameters under $\mathbb{P}$ are given by

$$
\boldsymbol{\psi} = [\lambda, \nu, \mu_1, \mu_2, d_2, \beta_1, \beta_2] \tag{17}
$$

Apart from λ, all of them are assumed to be nonnegative.

4.2 The VARG-B risk-neutral dynamics

I introduce an assumption on the Stochastic Discount Factor (SDF) that allows to obtain the risk neutral distribution and, therefore, to compute option prices. In specifying the SDF, I follow Majewski et al. (2015)[6]:

$$M_{t,t+1} = \frac{\exp(-\delta_2 y_{t+1} - \delta_{11} f_{1,t+1} - \delta_{12} f_{2,t+1})}{\mathbb{E}^{\mathbb{P}}[\exp(-\delta_2 y_{t+1} - \delta_{11} f_{1,t+1} - \delta_{12} f_{2,t+1})|\mathcal{F}_t]} \tag{18}$$

This SDF is a very flexible specification since it identifies two risk premia, i.e. δ_{11} and δ_{12} in addition to the usual equity premium, i.e. δ_2.
More precisely, δ_{11} compensates for the continuous volatility while δ_{12} compensates for the burst source of risk[7].

Proposition 3. *Under the model specification in (1) and (3)-(4) with the SDF specified as in (18), the VARG-B satisfies the no-arbitrage condition if and only if*

$$\delta_2 = \lambda + \frac{1}{2} \tag{19}$$

Proof. *See Appendix B*

Given the result in Proposition 3 and the market incompleteness, δ_{11} and δ_{12} are free parameters to be calibrated while δ_2 is considered as fixed. So, the no-arbitrage condition fixes the level of the equity risk premium, while both the continuous and burst variance risk premia are free parameters to be calibrated on the option prices sample.
The SDF in (18) belongs to the family of the exponential-affine factors. Indeed, it is possible to compute a recursion under the $\mathbb{Q}$ measure analogous to that given under $\mathbb{P}$.

Corollary 4. *Under $\mathbb{Q}$, the MGF for the VARG-B model has the following form:*

$$\varphi^{\mathbb{Q}}_{\delta_2,\delta_1}(t,T,z) = \mathbb{E}^{\mathbb{Q}}\left(e^{zy_{t,T}}|\mathcal{F}_t\right) = \exp\left(a^*_t + \mathbf{b}^{*\prime}_t \mathbf{f}_t\right) \tag{20}$$

[6]Corsi et al. (2013) introduce a SDF involving both the log-returns and Realized Volatility, applying a modified version of the standar discrete-time exponential affine SDF applied in Gourieroux and Monfort (2007). Majewski et al. (2015) present a more general and flexible version.

[7]Many authors (see Gagliardini et al., 2011,Christoffersen et al., 2013, Corsi et al., 2013 and Majewski et al., 2015) recognized the importance of variance-dependent risk premia in SDF in reconciling the time series properties of asset returns with the cross-section of option prices.

where:

$$a_s^* = a_{s+1}^* + \mathcal{A}(z - \delta_2, \mathbf{b}_{s+1}^* - \boldsymbol{\delta}_1) - \mathcal{A}(-\delta_2, -\boldsymbol{\delta}_1) \tag{21}$$

$$\mathbf{b}_s^* = \mathbf{b}_{s+1}^* + \mathcal{B}(z - \delta_2, \mathbf{b}_{s+1}^* - \boldsymbol{\delta}_1) - \mathcal{B}(-\delta_2, -\boldsymbol{\delta}_1) \tag{22}$$

with terminal conditions: $a_T^* = 0, \boldsymbol{b}_T^* = \boldsymbol{0}$ *and* $\mathcal{A}(\cdot,\cdot)$, $\mathcal{B}(\cdot,\cdot)$ *as in* (A.9) *and* (A.10), *respectively.*
Proof. *See Appendix C*

The comparison between the physical and the risk-neutral MGFs provides a one-to-one mapping between the set of parameters under $\mathbb{P}$ and the set of parameters under $\mathbb{Q}$.

Proposition 5. *Under the risk-neutral measure,* $\mathbb{Q}$ *the latent volatility still follows a VARG-B process with parameters*

$$\begin{array}{lll} d_2^{\mathbb{Q}} = \dfrac{d_2}{1 - y_2^* \mu_2} & \beta_1^{\mathbb{Q}} = \dfrac{\beta_1}{1 - y_1^* \mu_1} & \mu_1^{\mathbb{Q}} = \dfrac{\mu_1}{1 - y_1^* \mu_1} \\ \beta_2^{\mathbb{Q}} = \dfrac{\beta_2}{1 - y_2^* \mu_2} & \mu_2^{\mathbb{Q}} = \dfrac{\mu_2}{1 - y_2^* \mu_2} & \nu^{\mathbb{Q}} = \nu \end{array} \tag{23}$$

where $y_h^* = -\delta_{1h} - \delta_2 \lambda + \frac{\delta_2^2}{2}$ *for* $h = 1, 2$.

Proof. *See Appendix E*

The result proved in Proposition 5 and the analytical tractability of the VARG-B process simplify the computation of the risk-neutral MGF. In fact, the latter is obtained starting from the MGF under $\mathbb{P}$ and substituting the parameters under $\mathbb{P}$ with those under $\mathbb{Q}$.

Corollary 6. *Under* $\mathbb{Q}$ *the MGF for the VARG-B model has the same form as in (14) with equity risk premium*
$\lambda^{\mathbb{Q}} = -\frac{1}{2}$ *and* $d_2^{\mathbb{Q}}, \boldsymbol{\beta}^{\mathbb{Q}}, \mu_1^{\mathbb{Q}}, \mu_2^{\mathbb{Q}}, \nu^{\mathbb{Q}}$ *as in* (23).

Therefore, f_t is still a VARG-B process under the $\mathbb{Q}$ measure and the two risk premia δ_{11} and δ_{12} are the only parameters to be calibrated on option prices, as explained in

Section 4.4. Once the values of δ_{11} and δ_{12} are calibrated, all the parameters in (23) can be computed in closed-form following Corollary 6.

4.3 Data and stylized facts

The data used in this exercise consist of European call option prices written on the S&P500 Index for the same time period of data used in Section 3.3. The observations for the option prices range from January 5, 1996 to December 30, 2005. I only use Wednesday options data[8] yielding a total of 30061 observations. As it is customary in the literature (see Barone-Adesi et al., 2008, Corsi et al., 2013, Majewski et al., 2015), I filter out options with time to maturity less than 10 days or more than 360 days, implied volatility larger than 70% or prices less than 0.05. To perform the analysis, I split options into different categories according to time to maturity and moneyness. Moneyness (m) is defined as the underlying index level divided by the option strike price. A call option is defined as DOTM (deep out-of-the-money) if $\mathrm{m} \leq 0.94$, OTM if $0.94 < \mathrm{m} \leq 0.97$, ATM if $0.97 < \mathrm{m} \leq 1.03$, DITM if $1.03 < \mathrm{m} \leq 1.06$ and ITM if $\mathrm{m} > 1.06$. Based instead on the time to maturity (T), options are classified in four categories: short maturity if $\mathrm{T} \leq 50$, medium-short maturity if $50 < \mathrm{T} \leq 90$, medium-long if $90 < \mathrm{T} \leq 160$ and long maturity if $\mathrm{T} > 160$. Table 2 reports some descriptive statistics for the options classified by the moneyness and maturity definitions given above. From Panel A, the DOTM call options are heavly traded especially at longer maturity. According to the summary statistics in Panel B and Panel C, the observed implied volatility increases as option intrinsic value increases. Hence, ITM (DITM) calls are more expensive compared to OTM (DOTM) calls.

[8] The first motivation for using Wednesday data is that Wednesday is the day of the week least likely to be a holiday. Therefore, it is less likely than other days to be affected day-of-the-week effects (see Bakshi et al., 1997, Christoffersen et al., 2008).

Table 2: Summary statistics for the S&P500 Index option data. The observations refer to each Wednesday during January 5, 1996 to December 30, 2005. Panel A shows the number of option contracts sorted by moneyness and maturity. Panel B shows the average option prices classified by moneyness and maturity. Panel C shows the average implied volatilities sorted by moneyness and maturity. Implied volatilities are calculated using the Black & Scholes formula. T refers to the number of days to maturity while m represents the moneyness defined as the underlying index level divided by the option strike price.

Moneyness	$T \leq 50$	$50 < T \leq 90$	$90 < T \leq 160$	$T > 160$	All
Panel A: Number of Contracts					
$m \leq 0.94$	2419	2212	1426	2550	8607
$0.94 < m \leq 0.97$	2370	1341	540	665	4916
$0.97 < m \leq 1$	2940	1640	605	799	5984
$1 < m \leq 1.03$	2362	1115	446	622	4545
$1.03 < m \leq 1.06$	1345	472	259	247	2323
$m > 1.06$	1615	844	550	625	3634
All	13051	7624	3826	5508	30009
Panel B: Average Option Prices					
$m \leq 0.94$	0.93	3.28	7.08	17.19	7.37
$0.94 < m \leq 0.97$	3.72	11.17	23.35	46.51	13.70
$0.97 < m \leq 1$	12.37	25.23	40.67	65.73	25.88
$1 < m \leq 1.03$	29.28	42.04	56.23	82.08	42.28
$1.03 < m \leq 1.06$	53.39	65.26	81.13	103.61	64.23
$m > 1.06$	117.26	152.84	182.53	197.01	149.12
All	28.95	35.45	50.65	59.38	38.95
Panel C: Average Implied Volatility					
$m \leq 0.94$	0.1753	0.1570	0.1496	0.1475	0.1581
$0.94 < m \leq 0.97$	0.1407	0.1385	0.1486	0.1558	0.1430
$0.97 < m \leq 1$	0.1466	0.1503	0.1610	0.1625	0.1512
$1 < m \leq 1.03$	0.1601	0.1627	0.1650	0.1670	0.1622
$1.03 < m \leq 1.06$	0.1848	0.1791	0.1759	0.1776	0.1819
$m > 1.06$	0.2628	0.2359	0.2287	0.2042	0.2413
All	0.1716	0.1633	0.1662	0.1606	0.1668

4.4 The calibration of risk premia

Given the estimates of the parameters under the $\mathbb{P}$ measure obtained via the procedure described in Section 3.1, the risk premium parameters in (18) need to be calibrated to derive the risk-neutral dynamics.

Specifically, δ_2 is determined by the no-arbitrage condition in the Proposition 3, and δ_{11} and δ_{12} are calibrated on observed option prices. The purpose of the calibration is the selection of risk premia such that the model implied unconditional volatility under the risk-neutral measure matches the unconditional risk-neutral volatility. Notice that it is not possible to directly observe the latter, then I follow the same strategy used in Corsi et al. (2013). The market-observed implied volatility (IV) is used as an instrument to be matched with the model-generated IV since both depend on the volatility under $\mathbb{Q}$ measure. The two risk premia, δ_{11} and δ_{12}, are calibrated by minimising the loss function which measures the distance between the model generated IV for two options and the market IV corresponding to the same two options in the sample:

$$f(\delta_{11}, \delta_{12}) = \sqrt{\frac{1}{2}\left[(IV_1^{mkt} - IV_1^{mod})^2 + (IV_2^{mkt} - IV_2^{mod})^2\right]} \times 100 \tag{24}$$

where $IV_{i,t}^{mkt}$ is the market IV of the option i, $IV_{i,t}^{mod}$ is the IV computed from the model for the same option, with $i = 1, 2$. In order to deal with the risk premia calibration for the VARG-B model, I randomly select two ATM options from the most liquid ones, observed in two different days [9].

Then, I proceed in pricing options: first I map the parameters of the model estimated under $\mathbb{P}$ into the parameters under $\mathbb{Q}$ according to Proposition 5; second I approximate option prices by the COS method introduced by Fang and Oosterlee (2008), using the

[9] For the alternative models, ARG and HARG, the motivation behind the calibration is the same but, since the risk premium to be calibrated is only δ_{11}, I select just one option from the sample. To avoid the problem of a possible unfair comparison among models, I randomly choose one of the two options used to minimise the objective function in (24). I also calibrate both ARG and HARG models on the latter option (the option that is not randomly selected at the beginning), and the results are comparable in terms of pricing performance.

MGF formula in Proposition 2 with the parameters in Proposition 5. Finally, I compute the IVs for each model. As expected[10], both δ_{11} and δ_{12} are negative and equal to -0,8197 and -0,2386, respectively.

4.5 Option pricing performance

As it is customary in the literature, I analyse the option pricing performance of each model in terms of the Root Mean Square Error on the percentage IV:

$$RMSE_{IV} = \sqrt{\frac{1}{N}\sum_{i=1}^{N}(IV_i^{mkt} - IV_i^{mod})^2} \times 100 \tag{25}$$

where $IV_{i,t}^{mkt}$ is the market IV of option i, $IV_{i,t}^{mod}$ is the IV computed from the model for the same option, with $i = 1, 2, \ldots N$ and N is the total number of options in the sample. For completeness I report the performance results also for the Root Mean Square Error on option prices:

$$RMSE_P = \sqrt{\frac{1}{N}\sum_{i=1}^{N}(P_i^{mkt} - P_i^{mod})^2} \tag{26}$$

where $P_{i,t}^{mkt}$ is the market price of the option i, $P_{i,t}^{mod}$ is the price computed from the model of the option i, for $i = 1, 2, \ldots N$. The former metric represents an intuitive weighting of options across strikes and maturities. The latter gives more weight to options with high intrinsic value (DITM) and time value (longer maturity) but has the advantage of interpreting RMSE as $ errors.

Table 3 reports the global option pricing performance on the S&P500 call options from January 5, 1996 to December 30, 2005. The first row shows the absolute RMSE$_{IV}$ and the RMSE$_P$ for the VARG-B model, computed over the entire sample. The remaining rows display an indicator for the VARG-B relative performance with respect to the alternative

[10] Options are volatility-sensitive investments. They typically pay off in adverse states of nature, i.e. when the marginal utility of wealth is high. This means that such investment is negative-beta and, in turn, are characterised by negative risk premia.

models which is computed as the ratio between the RMSE_{IV} (RMSE_{P}) of the VARG-B and that of the ARG, HARG and LHARG-ARJ, respectively. Note that this indicator is a ratio between two loss functions, indeed a value less than one indicates an outperformance of the model set as the numerator, i.e. VARG-B model.

A comparison between the ARG and the VARG-B model illustrates the importance of a multifactor specification of volatility in pricing options. By comparing the VARG-B with the HARG model, I can shed some light on the importance of volatility bursts in fitting medium/long-term part of the implied volatility surface, especially for at-the-money options, with respect to the long-memory feature. Finally, a comparison between the LHARG-ARJ and the VARG-B model can clarify the role of volatility bursts or price jumps in causing the extreme price movements, highlighting the importance of volatility burst factor for the correct description of the volatility surface.

Table 3: Global option pricing performance. The first row shows the implied volatility root mean square error and the price root mean square error. RMSE_{IV} and RMSE_{P} are both expressed in percentage. The second and the third rows show the RMSE_{IV} and RMSE_{P} of the competitor models relative to the VARG-B. A ratio smaller than 1 indicates an outperformance of the VARG-B model. I use the parameter estimates from Table 1 and S&P500 call options from January 5, 1996 to December 30, 2005.

Model	RMSE_{IV}	RMSE_{P}
VARG-B	6.804	0.008
VARG-B/ARG	0.665	0.118
VARG-B/HARG	0.897	0.992
VARG-B/LHARG-ARJ	0.642	0.829

At first sight, the VARG-B model outperforms all the alternatives, both via RMSE_{IV} and RMSE_{P}. Specifically, looking at the RMSE_{IV} (RMSE_{P}), the VARG-B model improvement is about 35% (80%) over ARG and around 36% (18%) over LHARG-ARJ model. Instead, the VARG-B model has a performance very similar to that of the HARG, in terms of both loss functions.

In order to get a deeper understanding of the VARG-B pricing performance, Table 4 (Table 5) reports the results in terms of RMSE_{IV} (RMSE_{P}) disaggregated for different maturities and moneyness[11]. The results in Table 4 confirm that modelling the occurrence and the probability of having bursts in the volatility carries advantages over option evaluation. The VARG-B model offers a flexible volatility specification that translates in an increasing ability to capture the volatility smile.

Panel B of Table 4 compares the performance of VARG-B and ARG. It shows the advantage of providing an extraordinary burst factor in the volatility dynamics. Improvement for short maturities $T \leq 90$ and moneyness $1 < m \leq 1.06$ reaches more than 50% while for DOTM options at longer maturity ($T > 90$) the two models share approximately the same degree of underpricing.

The relative performance between VARG-B and HARG is displayed in Panel C of Table 4. In this comparison, I focus on the long-term part of the IV surface, where the persistence of the volatility process plays a fundamental role. Note that the heterogeneous structure for the volatility in the HARG model is introduced to mimic the long-memory characterising the volatility process. The advantage of volatility burst component yields accurate pricing also for longer maturities even if the improvement slowly trickles away as the time to maturity increases, remaining around 30% in the left part of the volatility surface ($m > 1.06$ and $T > 160$). This is a common feature of stochastic volatility option pricing models that do not allow for an enough degree of persistence and flexibility in the volatility dynamics. However, the VARG-B model is able to improve pricing along the DITM calls (corresponding to DOTM puts), which have proven difficult to price in the literature.

The results recorded in the Panel D of Table 4 favorite the VARG-B model with respect to a model with jumps in return dynamics, i.e. LHARG-ARJ model. The improvement increases moving from ATM to ITM call options, independently from the time to maturity

[11]The results recorded in Table 5 are in line with those reported in Table 4. For this reason, I will discuss only the pricing performance in terms of RMSE_{IV}.

dimension. The difference in perfomance suggests that extreme price movements can be considered as a by-product of volatility burst, in the spirit of COP intuition.

Indeed, the ability of the VARG-B model to reproduce higher level of persistence permits this more flexible model to outperform the HARG model and to improve pricing over the long-term part of the IV surface.

To summarise, the proposed VARG-B model is better able to reproduce the IV level for options along both the moneyness and the time to maturity dimensions. It improves upon all the alternative models, especially for DITM - ITM and short maturities. The volatility burst component appears to be an important and necessary ingredient for a more accurate option pricing and modelling of the IV surface.

5 Conclusion

In this paper, I propose an affine discrete-time model, labelled VARG-B, in which volatility experiences, in addition to frequent and small changes, periods of sudden and extreme movements, i.e. volatility bursts. The former changes are generated by a state variable, called continuous component while the volatility burst component generates the volatility changes due to extreme price movements. The total volatility is equal to the sum of these two independent factors which are both assumed as latent. The continuous component is modelled as an Autoregressive Gamma (ARG) while the volatility burst factor follows an Autoregressive Gamma Zero (ARG-Zero) process.

A great advantage of VARG-B is represented by the estimation strategy which allows to filter the time series of both the volatility components and to understand the relative contribution of both the factors to the total conditional variance of log-returns. The state space is augmented with a measurement equation that relates the latent volatility to an ex-post estimator of daily quadratic variation of the log-price process, i.e. Realized Volatility.

The VARG-B model leads to a fully analytic conditional Laplace transform (that is, exponential affine), which is particularly attractive for option pricing purposes. Indeed, the change of measure is performed adopting an exponentially affine stochastic discount factor which preserves all the analytical results in order to obtain closed-form option pricing formula.

The proposed VARG-B model is better able to reproduce the IV level for options along both the moneyness and the time to maturity dimensions with respect to some alternatives. The greatest improvement is registered for short-maturity options and for DITM and ITM call options. For these option categories, the VARG-B model outperforms alternative models and provides an improvement also for ATM options.

The more flexible volatility specification allows the VARG-B model to reproduce higher level of persistence, which improves the pricing along the long-term part of the IV surface.

From the evidence reported in this paper, the volatility burst component is an important and necessary ingredient for a more accurate option pricing and modelling of the IV surface.

The VARG-B model can be extended to include leverage effect in the volatility dynamics as well as a dependence between volatility components. I leave the possibility to study these features to future research.

Table 4: Option pricing performance via the percentage implied volatility root mean square error ($RMSE_{IV}$). The table shows the $RMSE_{IV}$ for the VARG-B model and the alternative models sorted by moneyness and maturity. A ratio smaller than 1 indicates an outperformance of the VARG-B model. I use the parameter estimates from Table 1 and S&P500 Call options from January 5, 1996 to December 30, 2005. T refers to the number of days to maturity while m represents the moneyness defined as the underlying index level divided by the option strike price.

Moneyness	T≤50	50<T≤90	90<T≤160	T>160
Panel A: VARG-B Implied Volatility RMSE				
m≤0.94	9.6488	8.6095	8.1006	7.9106
0.94<m≤0.97	7.0031	6.7457	6.3341	6.4132
0.97<m≤1	4.7940	5.1940	4.9464	5.7442
1<m≤1.03	4.0642	4.3103	4.8010	5.4614
1.03<m≤1.06	4.2700	4.3579	4.5079	4.7901
m>1.06	7.3998	10.1113	8.4294	5.4600
Panel B: VARG-B/ARG Implied Volatility RMSE				
m≤0.94	0.9183	0.9410	0.9926	1.0212
0.94<m≤0.97	0.8266	0.8186	0.8123	0.6974
0.97<m≤1	0.5540	0.5986	0.6014	0.6705
1<m≤1.03	0.4311	0.4520	0.5393	0.5790
1.03<m≤1.06	0.3988	0.4182	0.4714	0.4665
m>1.06	0.3981	0.6509	0.5851	0.4679
Panel C: VARG-B/HARG Implied Volatility RMSE				
m≤0.94	1.4156	1.5618	1.8791	1.9598
0.94<m≤0.97	0.8337	0.9565	1.2987	1.4700
0.97<m≤1	0.5591	0.7874	1.0531	1.3720
1<m≤1.03	0.5006	0.7016	0.9624	1.2590
1.03<m≤1.06	0.5187	0.7057	0.8528	1.0546
m>1.06	0.4962	0.8842	0.8612	0.6936
Panel D: VARG-B/LHARG-ARJ Implied Volatility RMSE				
m≤0.94	1.9480	2.0336	2.3302	2.0619
0.94<m≤0.97	1.5581	1.4904	1.4083	1.1642
0.97<m≤1	0.9533	1.0366	0.8976	0.8643
1<m≤1.03	0.6297	0.6949	0.7064	0.6306
1.03<m≤1.06	0.2841	0.3650	0.3723	0.3734
m>1.06	0.2670	0.4133	0.3633	0.2764

Table 5: Option pricing performance via the percentage price root mean square error ($RMSE_P$). The table shows the $RMSE_P$ for the VARG-B model and the alternative models sorted by moneyness and maturity. A ratio smaller than 1 indicates an outperformance of the VARG-B model. I use the parameter estimates from Table 1 and S&P500 Call options from January 5, 1996 to December 30, 2005. T refers to the number of days to maturity while m represents the moneyness defined as the underlying index level divided by the option strike price.

Moneyness	T≤50	50<T≤90	90<T≤160	T>160
Panel A: VARG-B Price RMSE				
m≤0.94	0.0036	0.0059	0.0092	0.0126
0.94<m≤0.97	0.0043	0.0077	0.0113	0.0154
0.97<m≤1	0.0043	0.0072	0.0107	0.0165
1<m≤1.03	0.0042	0.0068	0.0113	0.0187
1.03<m≤1.06	0.0039	0.0071	0.0136	0.0198
m>1.06	0.0038	0.0076	0.0154	0.0258
Panel B: VARG-B/ARG Price RMSE				
m≤0.94	0.0619	0.1116	0.1242	0.2055
0.94<m≤0.97	0.0914	0.1251	0.1501	0.2567
0.97<m≤1	0.0849	0.1600	0.1643	0.2232
1<m≤1.03	0.0960	0.1460	0.1366	0.2096
1.03<m≤1.06	0.0739	0.1097	0.1568	0.1900
m>1.06	0.0350	0.0493	0.0653	0.1126
Panel C: VARG-B/HARG Price RMSE				
m≤0.94	1.4191	1.4505	1.8192	1.7446
0.94<m≤0.97	0.7241	0.8498	1.1843	1.1635
0.97<m≤1	0.5222	0.7087	0.9124	1.0470
1<m≤1.03	0.4848	0.6507	0.8371	0.9601
1.03<m≤1.06	0.5153	0.7048	0.7863	0.8663
m>1.06	0.7075	0.8185	0.9667	1.2291
Panel D: VARG-B/LHARG-ARJ Price RMSE				
m≤0.94	2.6634	2.3463	1.9082	1.2849
0.94<m≤0.97	1.4804	1.3473	1.0030	0.6780
0.97<m≤1	0.8920	0.8903	0.6109	0.5086
1<m≤1.03	0.6544	0.6055	0.5061	0.4337
1.03<m≤1.06	0.4851	0.4568	0.4044	0.3399
m>1.06	0.4401	0.3709	0.3570	0.3463

A Proof of Proposition 1

The *Assumption 1* in Majewski et al. (2015) is the following:

$$\begin{aligned} & \mathbb{E}^{\mathbb{P}}\left[\exp(zy_{t+1} + \mathbf{b}'\mathbf{f}_{t+1} + \mathbf{c}'\mathbf{l}_{t+1})|\mathcal{F}_t, \mathcal{L}_t\right] \\ = \;& \exp\left[\mathcal{A}(z,\mathbf{b},\mathbf{c}) + \sum_{i=1}^{p}\mathcal{B}_i(z,\mathbf{b},\mathbf{c})'\cdot\mathbf{f}_{t+1-i} + \sum_{j=1}^{q}\mathcal{C}_j(z,\mathbf{b},\mathbf{c})'\cdot\mathbf{l}_{t+1-j}\right] \end{aligned} \tag{A.1}$$

for some functions $\mathcal{A}:\mathbb{R}\times\mathbb{R}^k\times\mathbb{R}^k\to\mathbb{R}$, $\mathcal{B}_i:\mathbb{R}\times\mathbb{R}^k\times\mathbb{R}^k\to\mathbb{R}^k$ and $\mathcal{C}_i:\mathbb{R}\times\mathbb{R}^k\times\mathbb{R}^k\to\mathbb{R}^k$, where $\mathbf{b},\mathbf{c}\in\mathbb{R}^k$ and $\cdot$ stands for the scalar product in $\mathbb{R}^k$. Indeed:

$$\begin{aligned} & \mathbb{E}^{\mathbb{P}}\left[\exp(zy_{t+1} + \mathbf{b}'\mathbf{f}_{t+1})|\mathcal{F}_t\right] \\ = \;& \exp\left[\mathcal{A}(z,\mathbf{b}) + \mathcal{B}(z,\mathbf{b})'\cdot\mathbf{f}_t\right] \end{aligned} \tag{A.2}$$

For the setup in Section 2.1, assumption (A.2) is satisfied with $\mathbf{l}_t = 0$ for $t = 1,\ldots,T$ and $p = 1$. Without loss of generality I assume $r_{t+1} = r$ for $t > 0$, since r_{t+1} is predetermined (that is, known at t).

To derive the expressions for $\mathcal{A}_t(z,\mathbf{b},\mathbf{c})$ and $\mathcal{B}_i(z,\mathbf{b},\mathbf{c})$, I write:

$$\begin{aligned} & \mathbb{E}^{\mathbb{P}}\left[\exp(zy_{t+1} + \mathbf{b}'\mathbf{f}_{t+1})|\mathcal{F}_t\right] \\ = \;& \mathbb{E}^{\mathbb{P}}\left[\exp(zr + z\lambda f_{t+1} + z\sqrt{f_{t+1}}\epsilon_{t+1} + b_1 f_{1,t+1} + b_2 f_{2,t+1})|\mathcal{F}_t\right] \\ = \;& e^{zr}\mathbb{E}^{\mathbb{P}}\left[\exp[(b_1 + z\lambda)f_{1,t+1} + (b_2 + z\lambda)f_{2,t+1} + z\sqrt{f_{t+1}}\epsilon_{t+1}]|\mathcal{F}_t\right] \\ = \;& e^{zr}\mathbb{E}^{\mathbb{P}}\left\{\exp\left[(b_1 + z\lambda)f_{1,t+1} + (b_2 + z\lambda)f_{2,t+1}\right]\right. \\ & \left.\times\mathbb{E}^{\mathbb{P}}\left[\exp\left[z\sqrt{f_{t+1}}\epsilon_{t+1}\right]\Big| f_{1,t+1}, f_{2,t+1}, \mathcal{F}_t\right]\Big|\mathcal{F}_t\right\} \end{aligned}$$

where $\mathbf{f}_{t+1} = (f_{1,t+1}, f_{2,t+1})'$.

To compute the inner expectation I now use the following property: if $Z \sim \mathcal{N}(0,1)$ and $Y = aZ$, then

$$\mathbb{E}\{\exp[xY]\} = \exp\left[\frac{1}{2}(xa)^2\right]$$

Hence:

$$
\begin{aligned}
& \mathbb{E}^{\mathbb{P}}\left[\exp(zy_{t+1}+\mathbf{b}'\mathbf{f}_{t+1})|\mathcal{F}_t\right] \\
= \; & e^{zr}\mathbb{E}^{\mathbb{P}}\left\{\exp\left[(b_1+z\lambda)f_{1,t+1}+(b_2+z\lambda)f_{2,t+1}+\frac{z^2}{2}f_{t+1}\;\right]\bigg|\,\mathcal{F}_t\right\} \\
= \; & e^{zr}\mathbb{E}^{\mathbb{P}}\left\{\exp\left[(b_1+z\lambda)f_{1,t+1}+(b_2+z\lambda)f_{2,t+1}+\frac{z^2}{2}f_{1,t+1}+\frac{z^2}{2}f_{2,t+1}\;\right]\bigg|\,\mathcal{F}_t\right\} \\
= \; & e^{zr}\mathbb{E}^{\mathbb{P}}\left\{\exp\left[x_1(z,\mathbf{b})f_{1,t+1}+x_2(z,\mathbf{b})f_{2,t+1}\right]|\,\mathcal{F}_t\right\}
\end{aligned}
$$

where:

$$
x_1(z,\mathbf{b}) \;=\; b_1+z\lambda+\frac{z^2}{2} \tag{A.3}
$$

$$
x_2(z,\mathbf{b}) \;=\; b_2+z\lambda+\frac{z^2}{2} \tag{A.4}
$$

In what follows I will sometimes simplify the notation using x_1 (resp. x_2) instead of $x_1(z,\mathbf{b})$ (resp. $x_2(x,\mathbf{b})$). I now use the following property of the noncentral Gamma-Zero distribution: if $Z\sim\gamma_0(\theta,\mu)$, then

$$
\mathbb{E}[\exp(xZ)]=\exp\left[\frac{x\mu}{1-x\mu}\,\theta\right].
$$

Since $f_{2,t+1}|\mathcal{F}_t\sim\gamma_0(d_2+\beta_2 f_{2,t},\mu_2)$, defining $\theta_{2t}=d_2+\beta_2 f_{2,t}$, I get:

$$
\begin{aligned}
& \mathbb{E}^{\mathbb{P}}\left[\exp(zy_{t+1}+\mathbf{b}'\mathbf{f}_{t+1})|\mathcal{F}_t\right] \\
= \; & e^{zr}\mathbb{E}^{\mathbb{P}}\left\{\exp[x_1(z,\mathbf{b})f_{1,t+1}]\mathbb{E}^{\mathbb{P}}\left[\exp\left(x_2(z,\mathbf{b})f_{2,t+1}\right)|\,f_{1,t+1},\mathcal{F}_t\right]\Big|\,\mathcal{F}_t\right\} \\
= \; & e^{zr\frac{x_2\mu_2}{1-x_2\mu_2}\theta_{2t}}\mathbb{E}^{\mathbb{P}}\left\{\exp\left[x_1 f_{1,t+1}\right]|\,\mathcal{F}_t\right\} \\
= \; & \mathrm{e}^{zr+V_2(x_2,\mu_2)\theta_{2t}}\mathbb{E}^{\mathbb{P}}\left\{\exp\left[x_1 f_{1,t+1}\right]|\,\mathcal{F}_t\right\}
\end{aligned}
$$

where:

$$
V_2[x_2,\mu_2] \;=\; \frac{x_2(z,\mathbf{b})\mu_2}{1-x_2(z,\mathbf{b})\mu_2} \tag{A.5}
$$

I now use the following property of the noncentral Gamma distribution: if $Z \sim \gamma_\nu(\theta, \mu)$, then

$$\mathbb{E}[\exp(xZ)] = \exp\left[\frac{x\mu}{1-x\mu}\,\theta - \nu\log(1-x\mu)\right].$$

Since $f_{1,t+1}|\mathcal{F}_t \sim \gamma_\nu(\beta_1 f_{1,t}, \mu_1)$, defining $\theta_{1t} = \beta_1 f_{1,t}$, I get:

$$\begin{aligned}
&\mathbb{E}^{\mathbb{P}}\left[\exp(zy_{t+1} + \mathbf{b}'\mathbf{f}_{t+1})|\mathcal{F}_t\right] \\
&= \exp\left\{zr + V_2(x_2,\mu_2)\theta_{2t} - \nu\log(1-x_1\mu_1) + \frac{x_1\mu_1}{1-x_1\mu_1}\theta_{1t}\right\} \\
&= \exp\left\{zr - \nu W_1(x_1,\mu_1) + V_1(x_1,\mu_1)\theta_{1t} + V_2(x_2,\mu_2)\theta_{2t}\right\} \qquad \text{(A.6)}
\end{aligned}$$

where

$$W_1[x_1,\mu_1] = \log[1 - x_1(z,\mathbf{b})\mu_1] \qquad \text{(A.7)}$$

$$V_1[x_1,\mu_1] = \frac{x_1(z,\mathbf{b})\mu_1}{1 - x_1(z,\mathbf{b})\mu_1} \qquad \text{(A.8)}$$

Substituting the expressions for non-centrality parameters in (A.6) and collecting terms, it is easy to check that Assumption A.2 is satisfied, with:

$$\mathcal{A}(z,\mathbf{b}) = zr - \nu W_1(x_1,\mu_1) + V_2(x_2,\mu_2)d_2 \qquad \text{(A.9)}$$

$$\mathcal{B}(z,\mathbf{b})' = [V_1(x_1,\mu_1)\ ,\ V_2(x_2,\mu_2)]\,\boldsymbol{\beta} \qquad \text{(A.10)}$$

where $\boldsymbol{\beta} = (\beta_1, \beta_2)'$.

B Proof of Proposition 3

The assumed SDF is

$$M_{t,t+1} = \frac{\exp(-\delta_2 y_{t+1} - \delta_{11} f_{1,t+1} - \delta_{12} f_{2,t+1})}{\mathbb{E}^{\mathbb{P}}[\exp(-\delta_2 y_{t+1} - \delta_{11} f_{1,t+1} - \delta_{12} f_{2,t+1})|\mathcal{F}_t]} \qquad \text{(B.11)}$$

The no-arbitrage conditions are

$$\mathbb{E}^{\mathbb{P}}[M_{s,s+1}|\mathcal{F}_s] = 1 \qquad \text{for} \quad s \in \mathbb{N} \tag{B.12}$$

$$\mathbb{E}^{\mathbb{P}}[M_{s,s+1}e^{y_{s+1}}|\mathcal{F}_s] = e^r \qquad \text{for} \quad s \in \mathbb{N} \tag{B.13}$$

The first condition is satisfied by definition of $M_{t,t+1}$.

Let $\delta_1 = (\delta_{11}, \delta_{12})'$. To enforce no arbitrage, I use *Proposition 2* in Majewski et al. (2015), which shows that the second condition is equivalent to:

$$\begin{aligned} \mathcal{A}(1-\delta_2, -\delta_1) &= r + \mathcal{A}(-\delta_2, -\delta_1) \\ \mathcal{B}(1-\delta_2, -\delta_1) &= \mathcal{B}(-\delta_2, -\delta_1) \end{aligned}$$

These equalities are implied by

$$\begin{aligned} x_1(1-\delta_2, -\delta_1) &= x_1(-\delta_2, -\delta_1) \\ x_2(1-\delta_2, -\delta_1) &= x_2(-\delta_2, -\delta_1). \end{aligned}$$

For this to hold, it is easy to check that it is sufficient to impose

$$\delta_2 = \lambda + \frac{1}{2} \tag{B.14}$$

C Proof of Corollary 4

Let $y_{t,T} = \log(S_T/S_t)$ I have to show that:

$$\varphi^{\mathbb{Q}}_{\delta_2,\delta_1}(t,T,z) = \mathbb{E}^{\mathbb{Q}}\left(e^{zy_{t,T}}|\mathcal{F}_t\right) = \exp\left(a^*_t + \mathbf{b}^{*\prime}_t \mathbf{f}_t\right) \tag{C.15}$$

where:

$$a_s^* = a_{s+1}^* + \mathcal{A}(z - \delta_2, \mathbf{b}_{s+1}^* - \boldsymbol{\delta_1}) - \mathcal{A}(-\delta_2, -\boldsymbol{\delta_1}) \tag{C.16}$$

$$\mathbf{b}_s^* = \mathbf{b}_{s+1}^* + \mathcal{B}(z - \delta_2, \mathbf{b}_{s+1}^* - \boldsymbol{\delta_1}) - \mathcal{B}(-\delta_2, -\boldsymbol{\delta_1}) \tag{C.17}$$

subject to the terminal conditions:

$$a_T^* = 0, \quad \boldsymbol{b}_T^* = \mathbf{0}$$

The above relation is derived using the expression for the SDF in (18) repeatedly and using the tower law of conditional expectation:

$$\begin{aligned}
&\varphi^{\mathbb{Q}}_{\delta_2,\boldsymbol{\delta_1}}(t,T,z) \\
&= \mathbb{E}^{\mathbb{Q}}\left[e^{zy_{t,T}}|\mathcal{F}_t\right] \\
&= \mathbb{E}^{\mathbb{P}}\left[M_{t,t+1}\dots M_{T-1,T}e^{zy_{t,T}}|\mathcal{F}_t\right] \\
&= \mathbb{E}^{\mathbb{P}}\left[M_{t,t+1}\dots M_{T-2,T-1}e^{zy_{t,T-1}}\mathbb{E}^{\mathbb{P}}\left[M_{T-1,T}e^{y_T}|\mathcal{F}_{T-1}\right]|\mathcal{F}_t\right] \\
&= \mathbb{E}^{\mathbb{P}}\left[M_{t,t+1}\dots M_{T-2,T-1}e^{zy_{t,T-1}}\mathbb{E}^{\mathbb{P}}\left[\frac{e^{-\delta_2 y_T-\delta_{11}f_{1,T}-\delta_{12}f_{2,T}+zy_T}}{\mathbb{E}^{\mathbb{P}}\left[e^{-\delta_2 y_T-\delta_{11}f_{1,T}-\delta_{12}f_{2,T}}|\mathcal{F}_{T-1}\right]}|\mathcal{F}_{T-1}\right]|\mathcal{F}_t\right] \\
&= \mathbb{E}^{\mathbb{P}}\left[M_{t,t+1}\dots M_{T-2,T-1}e^{zy_{t,T-1}-\mathcal{A}(-\delta_2,-\delta_1)-\mathcal{B}(-\delta_2,-\boldsymbol{\delta_1})\boldsymbol{f}_{T-1}}\mathbb{E}^{\mathbb{P}}\left[e^{(z-\delta_2)y_T-\delta_1\boldsymbol{f}_T}|\mathcal{F}_{T-1}\right]|\mathcal{F}_t\right] \\
&= \mathbb{E}^{\mathbb{P}}\left[M_{t,t+1}\dots M_{T-2,T-1}e^{zy_{t,T-1}-\mathcal{A}(-\delta_2,-\delta_1)-\mathcal{B}(-\delta_2,-\delta_1)\boldsymbol{f}_{T-1}+\mathcal{A}(z-\delta_2,-\delta_1)+\mathcal{B}(z-\delta_2,-\delta_1)\boldsymbol{f}_{T-1}}|\mathcal{F}_t\right] \\
&= \mathbb{E}^{\mathbb{P}}\left[M_{t,t+1}\dots M_{T-2,T-1}e^{zy_{t,T-1}+a_{T-1}^*+b_{T-1}^*\boldsymbol{f}_{T-1}}|\mathcal{F}_t\right] \\
&= \mathbb{E}^{\mathbb{P}}\left[M_{t,t+1}\dots M_{T-3,T-2}e^{zy_{t,T-2}+a_{T-1}^*}\mathbb{E}^{\mathbb{P}}\left[M_{T-2,T-1}e^{zy_{T-1}+b_{T-1}^*\boldsymbol{f}_{T-1}}|\mathcal{F}_{T-2}\right]|\mathcal{F}_t\right] \\
&= \mathbb{E}^{\mathbb{P}}\left[M_{t,t+1}\dots M_{T-3,T-2}e^{zy_{t,T-2}+a_{T-1}^*-\mathcal{A}(-\delta_2,-\delta_1)-\mathcal{B}(-\delta_2,-\delta_1)\boldsymbol{f}_{T-2}+\mathcal{A}(z-\delta_2,\mathbf{b}_{T-1}^*-\delta_1)+\mathcal{B}(z-\delta_2,\mathbf{b}_{T-1}^*-\delta_1)\boldsymbol{f}_{T-2}}|\mathcal{F}_t\right] \\
&= \dots \\
&= \mathrm{e}^{(a_t^*+\mathbf{b}_t^{*\prime}\mathbf{f}_t)}
\end{aligned}$$

I now specialize these expression for the setup outlined in Section 2.1. Consider equation (C.16). Using (A.9), I get

$$a^*_s = a^*_{s+1} + zr - \nu(W^*_{1,s+1} - W^y_1) + d_2(V^*_{2,s+1} - V^y_2) \tag{C.18}$$

where:

$$\begin{aligned}
x^*_{h,s+1} &= x_h(z - \delta_2, \boldsymbol{b}^*_{s+1} - \boldsymbol{\delta}_1), \quad h = 1,2 \\
y^*_h &= x_h(-\delta_2, -\boldsymbol{\delta}_1) = -\delta_{1h} - \delta_2\lambda + \frac{\delta_2^2}{2}, \quad h = 1,2 \\
V^*_{h,s+1} &= V_h(x^*_{h,s+1}, \mu_h), \quad h = 1,2 \\
V^y_h &= V_h(y^*_h, \mu_h), \quad h = 1,2 \\
W^*_{1,s+1} &= W_1(x^*_{1,s+1}, \mu_1) \\
W^y_1 &= W_1(y^*_1, \mu_1)
\end{aligned}$$

Using (A.10), equation (C.17) becomes:

$$\mathbf{b}^{*\prime}_s \;=\; \mathbf{b}^{*\prime}_{s+1} + (V^*_{1,s+1} - V^y_1\ ,\ V^*_{2,s+1} - V^y_2)\boldsymbol{\beta} \tag{C.19}$$

D Proof of Proposition 2

To compute the MGF of $y_{t,T}$ under $\mathbb{P}$, I simply need to plug $\delta_2 = 0$ and $\boldsymbol{\delta_1} = \mathbf{0}$ in the expression of $\varphi^{\mathbb{Q}}_{\delta_2,\delta_1}(t, T, z)$ in (C.15):

$$\varphi^{\mathbb{Q}}_{0,0}(t, T, z) = \mathbb{E}^{\mathbb{P}}[e^{zy_{t,T}}|\mathcal{F}_t] = exp\left(a_t + \mathbf{b}'_t\mathbf{f}_t\right) \tag{D.20}$$

where

$$\begin{aligned}
a_s &= a_{s+1} + zr - \nu W_{1,s+1} + d_2 V_{2,s+1} && \text{(D.21)} \\
\mathbf{b}'_s &= \mathbf{b}'_{s+1} + (V_{1,s+1}, V_{2,s+1})\boldsymbol{\beta} && \text{(D.22)}
\end{aligned}$$

with

$$x_{h,s+1} = x_h(z, \mathbf{b}_{s+1}) = \mathbf{b}_{s+1} + z\lambda + \frac{z^2}{2}, \quad h = 1,2$$

and

$$\begin{aligned} V_{h,s+1} &= V_h(x_{h,s+1}, \mu_h) = \frac{x_{h,s+1}\mu_h}{1 - x_{h,s+1}\mu_h}, \quad h = 1,2 \\ W_{1,s+1} &= W_1(x_{1,s+1}, \mu_1) = \log(1 - x_{1,s+1}\mu_1) \end{aligned}$$

subject to the initial conditions:

$$a_T = 0, \quad \mathbf{b}'_T = 0$$

E Proof of Proposition 5

The MGFs $\varphi^{\mathbb{Q}}_{\delta_2,\delta_1}(t,T,z)$ and $\varphi^{\mathbb{P}}_{0,\mathbf{0}}(t,T,z)$ derived above depend on the parameters under $\mathbb{P}$, $\boldsymbol{\psi}$ defined in (17), and on the risk premium parameters $\boldsymbol{\delta} = (\delta_2, \delta_1')'$ introduced in the SDF (18). I now show that the MGF under $\mathbb{Q}$ can be rewritten as the MGF under $\mathbb{P}$ using a new set of parameters $\boldsymbol{\psi}^{\mathbb{Q}}$ i.e. the risk-neutral ones

$$\boldsymbol{\psi}^{\mathbb{Q}} = [\lambda^{\mathbb{Q}}, \nu^{\mathbb{Q}}, \mu_1^{\mathbb{Q}}, \mu_2^{\mathbb{Q}}, d_2^{\mathbb{Q}}, \boldsymbol{\beta}^{\mathbb{Q}}] \tag{E.23}$$

To derive the expression of $\boldsymbol{\psi}^{\mathbb{Q}}$ as a function of $\boldsymbol{\psi}$ and $\boldsymbol{\delta}$, I match the parameters using the identity:

$$\varphi^{\mathbb{Q}}_{\delta_2,\delta_1}(t,T,z;\boldsymbol{\psi},\boldsymbol{\delta}) = \varphi^{\mathbb{P}}_{0,\mathbf{0}}(t,T,z;\boldsymbol{\psi}^{\mathbb{Q}}) \tag{E.24}$$

It is useful to denote

$$\begin{aligned} x^{\mathbb{Q}}_{h,s+1} &= x_h(z, \boldsymbol{b}^*_{s+1}; \boldsymbol{\psi}^{\mathbb{Q}}), \quad h = 1,2 \\ V^{\mathbb{Q}}_{h,s+1} &= V_h(x^{\mathbb{Q}}_{h,s+1}, \mu^{\mathbb{Q}}_h), \quad h = 1,2 \\ W^{\mathbb{Q}}_{1,s+1} &= W_1(x^{\mathbb{Q}}_{1,s+1}, \mu^{\mathbb{Q}}_1) \end{aligned}$$

For (E.24) to hold, (C.18) needs to be matched with (15) and (C.19) with (16) , where (15) and (16) are evaluated at $V^Q_{1,s+1}$, $V^Q_{2,s+1}$ and $W^Q_{1,s+1}$. Note that since I start from the same initial conditions (E.24) requires

$$\begin{aligned} \nu(W^*_{1,s+1} - W^y_1) &= \nu^Q W^Q_{1,s+1} \quad &\text{(E.25)} \\ d_2(V^*_{2,s+1} - V^y_2) &= d^Q_2 V^Q_{2,s+1} \quad &\text{(E.26)} \\ (V^*_{1,s+1} - V^y_1\ ,\ V^*_{2,s+1} - V^y_2)\boldsymbol{\beta} &= (V^Q_{1,s+1}\ ,\ V^Q_{2,s+1})\boldsymbol{\beta}^Q \quad &\text{(E.27)} \end{aligned}$$

for all s.

Consider (E.25). This requires

$$\nu[\log(1 - x^*_{1,s+1}\mu_1) - \log(1 - y^*_1\mu_1)] = \nu^Q \log(1 - x^Q_{1,s+1}\mu^Q_1)$$

Sufficient conditions for this equality to hold are

$$\nu^Q = \nu, \quad \mu^Q_1 = \frac{\mu_1}{1 - y^*_1\mu_1} \quad \text{and} \quad x^Q_{1,s+1} = x^*_{1,s+1} - y^*_1.$$

In turn, it can be checked that the latter equality is valid if I pose

$$\lambda^Q = -\frac{1}{2}.$$

Note that under these conditions I also have $x^Q_{2,s+1} = x^*_{2,s+1} - y^*_2$.

Now turn to (E.26):

$$d_2\left(\frac{x^*_{2,s+1}\mu_2}{1 - x^*_{2,s+1}\mu_2} - \frac{y^*_2\mu_2}{1 - y^*_2\mu_2}\right) = d^Q_2 \frac{x^Q_{2,s+1}\mu^Q_2}{1 - x^Q_{2,s+1}\mu^Q_2}.$$

If I substitute for $x^Q_{2,s+1}$ the expression obtained above, I get:

$$d^Q_2 = \frac{d_2}{1 - y^*_2\mu_2}$$

Its validity is guaranteed if $\mu_2^{\mathbb{Q}}$ is:

$$\mu_2^{\mathbb{Q}} = \frac{\mu_2}{1 - y_2^* \mu_2}$$

Note that these solutions also imply that $V_{2,s+1}^{\mathbb{Q}} = (1 - y_2^* \mu_2)(V_{2,s+1}^* - V_2^y)$

Finally, I turn to (E.27) which implies:

$$\beta_h^{\mathbb{Q}} = \frac{\beta_h}{1 - y_h^* \mu_h}, \quad h = 1, 2$$

Note that under this condition $V_{1,s+1}^{\mathbb{Q}} = (1 - y_1^* \mu_1)(V_{1,s+1}^* - V_1^y)$.

References

Akaike, H. (1998). Information theory and an extension of the maximum likelihood principle. In *Selected Papers of Hirotugu Akaike*, pp. 199–213. Springer.

Alitab, D., G. Bormetti, F. Corsi, and A. A. Majewski (2020). A jump and smile ride: Jump and variance risk premia in option pricing. *Journal of Financial Econometrics 18*(1), 121–157.

Andersen, T. G. and T. Bollerslev (1998). Answering the skeptics: Yes, standard volatility models do provide accurate forecasts. *International economic review*, 885–905.

Andersen, T. G., T. Bollerslev, and F. X. Diebold (2007). Roughing it up: Including jump components in the measurement, modeling, and forecasting of return volatility. *The Review of Economics and Statistics 89*(4), 701–720.

Bakshi, G., C. Cao, and Z. Chen (1997). Empirical performance of alternative option pricing models. *The Journal of finance 52*(5), 2003–2049.

Barone-Adesi, G., R. F. Engle, and L. Mancini (2008). A GARCH option pricing model with filtered historical simulation. *Review of Financial Studies 21*(3), 1223–1258.

Biais, B., L. Glosten, and C. Spatt (2005). Market microstructure: A survey of microfoundations, empirical results, and policy implications. *Journal of Financial Markets 8*(2), 217–264.

Caporin, M., E. Rossi, and P. S. de Magistris (2017). Chasing volatility: A persistent multiplicative error model with jumps. *Journal of Econometrics 198*(1), 122–145.

Caporin, M., E. Rossi, P. S. de Magistris, et al. (2015). Volatility jumps and their economic determinants. *Journal of Financial Econometrics 14*(1), 29–80.

Christensen, K., R. C. Oomen, and M. Podolskij (2014). Fact or friction: Jumps at ultra high frequency. *Journal of Financial Economics 114*(3), 576–599.

Christoffersen, P., S. Heston, and K. Jacobs (2013). Capturing option anomalies with a variance-dependent pricing kernel. *Review of Financial Studies 26*(8), 1963–2006.

Christoffersen, P., K. Jacobs, C. Ornthanalai, and Y. Wang (2008). Option valuation with long-run and short-run volatility components. *Journal of Financial Economics 90*(3), 272–297.

Corsi, F. (2009). A simple approximate long-memory model of realized volatility. *Journal of Financial Econometrics*, nbp001.

Corsi, F., N. Fusari, and D. La Vecchia (2013). Realizing smiles: Options pricing with realized volatility. *Journal of Financial Economics 107*(2), 284–304.

Corsi, F., D. Pirino, and R. Reno (2010). Threshold bipower variation and the impact of jumps on volatility forecasting. *Journal of Econometrics 159*(2), 276–288.

Cox, J. C., J. E. Ingersoll Jr, and S. A. Ross (1985). A theory of the term structure of interest rates. *Econometrica: Journal of the Econometric Society*, 385–407.

Engle, R. F. and G. M. Gallo (2006). A multiple indicators model for volatility using intra-daily data. *Journal of Econometrics 131*(1), 3–27.

Fang, F. and C. W. Oosterlee (2008). A novel pricing method for european options based on fourier-cosine series expansions. *SIAM Journal on Scientific Computing 31*(2), 826–848.

Gagliardini, P., C. Gourieroux, and E. Renault (2011). Efficient derivative pricing by the extended method of moments. *Econometrica 79*(4), 1181–1232.

Gourieroux, C. and J. Jasiak (2006). Autoregressive gamma processes. *Journal of Forecasting 25*(2), 129–152.

Gourieroux, C. and A. Monfort (2007). Econometric specification of stochastic discount factor models. *Journal of Econometrics 136*(2), 509–530.

Madhavan, A. (2000). Market microstructure: A survey. *Journal of financial markets 3*(3), 205–258.

Majewski, A. A., G. Bormetti, and F. Corsi (2015). Smile from the past: A general option pricing framework with multiple volatility and leverage components. *Journal of Econometrics*.

McAleer, M. and M. C. Medeiros (2008). Realized volatility: A review. *Econometric Reviews 27*(1-3), 10–45.

Merton, R. C. (1976). Option pricing when underlying stock returns are discontinuous. *Journal of financial economics 3*(1-2), 125–144.

Monfort, A., F. Pegoraro, J.-P. Renne, and G. Roussellet (2014). Recursive discrete-time affine processes and asset pricing. *Technical report, mimeo.*.

Schwarz, G. et al. (1978). Estimating the dimension of a model. *The annals of statistics 6*(2), 461–464.

RECENTLY PUBLISHED "TEMI" (*)

———————

(*) Requests for copies should be sent to:
Banca d'Italia – Servizio Studi di struttura economica e finanziaria – Divisione Biblioteca e Archivio storico – Via Nazionale, 91 – 00184 Rome – (fax 0039 06 47922059). They are available on the Internet www.bancaditalia.it.

2019

ALBANESE G., M. CIOFFI and P. TOMMASINO, *Legislators' behaviour and electoral rules: evidence from an Italian reform,* European Journal of Political Economy, v. 59, pp. 423-444, **WP 1135 (September 2017).**

APRIGLIANO V., G. ARDIZZI and L. MONTEFORTE, *Using the payment system data to forecast the economic activity,* International Journal of Central Banking, v. 15, 4, pp. 55-80, **WP 1098 (February 2017).**

ARNAUDO D., G. MICUCCI, M. RIGON and P. ROSSI, *Should I stay or should I go? Firms' mobility across banks in the aftermath of the financial crisis,* Italian Economic Journal / Rivista italiana degli economisti, v. 5, 1, pp. 17-37, **WP 1086 (October 2016).**

BASSO G., F. D'AMURI and G. PERI, *Immigrants, labor market dynamics and adjustment to shocks in the euro area,* IMF Economic Review, v. 67, 3, pp. 528-572, **WP 1195 (November 2018).**

BATINI N., G. MELINA and S. VILLA, *Fiscal buffers, private debt, and recession: the good, the bad and the ugly,* Journal of Macroeconomics, v. 62, **WP 1186 (July 2018).**

BURLON L., A. NOTARPIETRO and M. PISANI, *Macroeconomic effects of an open-ended asset purchase programme,* Journal of Policy Modeling, v. 41, 6, pp. 1144-1159, **WP 1185 (July 2018).**

BUSETTI F. and M. CAIVANO, *Low frequency drivers of the real interest rate: empirical evidence for advanced economies,* International Finance, v. 22, 2, pp. 171-185, **WP 1132 (September 2017).**

CAPPELLETTI G., G. GUAZZAROTTI and P. TOMMASINO, *Tax deferral and mutual fund inflows: evidence from a quasi-natural experiment,* Fiscal Studies, v. 40, 2, pp. 211-237, **WP 938 (November 2013).**

CARDANI R., A. PACCAGNINI and S. VILLA, *Forecasting with instabilities: an application to DSGE models with financial frictions,* Journal of Macroeconomics, v. 61, **WP 1234 (September 2019).**

CHIADES P., L. GRECO, V. MENGOTTO, L. MORETTI and P. VALBONESI, *Fiscal consolidation by intergovernmental transfers cuts? The unpleasant effect on expenditure arrears,* Economic Modelling, v. 77, pp. 266-275, **WP 1076 (July 2016).**

CIANI E., F. DAVID and G. DE BLASIO, *Local responses to labor demand shocks: a re-assessment of the case of Italy,* Regional Science and Urban Economics, v. 75, pp. 1-21, **WP 1112 (April 2017).**

CIANI E. and P. FISHER, *Dif-in-dif estimators of multiplicative treatment effects,* Journal of Econometric Methods, v. 8. 1, pp. 1-10, **WP 985 (November 2014).**

CIAPANNA E. and M. TABOGA, *Bayesian analysis of coefficient instability in dynamic regressions,* Econometrics, MDPI, Open Access Journal, v. 7, 3, pp.1-32, **WP 836 (November 2011).**

COLETTA M., R. DE BONIS and S. PIERMATTEI, *Household debt in OECD countries: the role of supply-side and demand-side factors,* Social Indicators Research, v. 143, 3, pp. 1185–1217, **WP 989 (November 2014).**

COVA P., P. PAGANO and M. PISANI, *Domestic and international effects of the Eurosystem Expanded Asset Purchase Programme,* IMF Economic Review, v. 67, 2, pp. 315-348, **WP 1036 (October 2015).**

ERCOLANI V. and J. VALLE E AZEVEDO, *How can the government spending multiplier be small at the zero lower bound?,* Macroeconomic Dynamics, v. 23, 8. pp. 3457-2482, **WP 1174 (April 2018).**

FERRERO G., M. GROSS and S. NERI, *On secular stagnation and low interest rates: demography matters,* International Finance, v. 22, 3, pp. 262-278, **WP 1137 (September 2017).**

FOA G., L. GAMBACORTA, L. GUISO and P. E. MISTRULLI, *The supply side of household finance,* Review of Financial Studies, v.32, 10, pp. 3762-3798, **WP 1044 (November 2015).**

GERALI A. and S. NERI, *Natural rates across the Atlantic,* Journal of Macroeconomics, v. 62, article 103019, **WP 1140 (September 2017).**

GIORDANO C., M. MARINUCCI and A. SILVESTRINI, *The macro determinants of firms' and households' investment: evidence from Italy,* Economic Modelling, v. 78, pp. 118-133, **WP 1167 (March 2018).**

GOMELLINI M., D. PELLEGRINO and F. GIFFONI, *Human capital and urban growth in Italy,1981-2001,* Review of Urban & Regional Development Studies, v. 31, 2, pp. 77-101, **WP 1127 (July 2017).**

LIBERATI D. and M. LOBERTO, *Taxation and housing markets with search frictions,* Journal of Housing Economics, v. 46, article 101632, **WP 1105 (March 2017).**

MAGRI S., *Are lenders using risk-based pricing in the Italian consumer loan market? The effect of the 2008 crisis,* Journal of Credit Risk, v. 15, 1, pp. 27-65, **WP 1164 (January 2018).**

MERCATANTI A., T. MAKINEN and A. SILVESTRINI, *The role of financial factors for european corporate investment,* Journal of International Money and Finance, v. 96, pp. 246-258, **WP 1148 (October 2017).**

MIGLIETTA A., C. PICILLO and M. PIETRUNTI, *The impact of margin policies on the Italian repo market,* The North American Journal of Economics and Finance, v. 50, **WP 1028 (October 2015).**

MONTEFORTE L. and V. RAPONI, *Short-term forecasts of economic activity: are fortnightly factors useful?,* Journal of Forecasting, v. 38, 3, pp. 207-221, **WP 1177 (June 2018).**

NERI S. and A. NOTARPIETRO, *Collateral constraints, the zero lower bound, and the debt–deflation mechanism,* Economics Letters, v. 174, pp. 144-148, **WP 1040 (November 2015).**

PANCRAZI R. and M. PIETRUNTI, *Natural expectations and home equity extraction,* Journal of Housing Economics, v. 46, 4, **WP 984 (November 2014).**

PEREDA FERNANDEZ S., *Teachers and cheaters. Just an anagram?*, Journal of Human Capital, v. 13, 4, pp. 635-669, **WP 1047 (January 2016).**

RIGGI M., *Capital destruction, jobless recoveries, and the discipline device role of unemployment,* Macroeconomic Dynamics, v. 23, 2, pp. 590-624, **WP 871 (July 2012).**

2020

ALESSANDRI P. and M. BOTTERO, *Bank lending in uncertain times,* R European Economic Review, V. 128, **WP 1109 (April 2017).**

ANTUNES A. and V. ERCOLANI, *Public debt expansions and the dynamics of the household borrowing constraint,* Review of Economic Dynamics, v. 37, pp. 1-32, **WP 1268 (March 2020).**

ARDUINI T., E. PATACCHINI and E. RAINONE, *Treatment effects with heterogeneous externalities,* Journal of Business & Economic Statistics, , v. 38, 4, pp. 826-838, **WP 974 (October 2014).**

BOLOGNA P., A. MIGLIETTA and A. SEGURA, *Contagion in the CoCos market? A case study of two stress events,* International Journal of Central Banking, v. 16, 6, pp. 137-184, **WP 1201 (November 2018).**

BOTTERO M., F. MEZZANOTTI and S. LENZU, *Sovereign debt exposure and the Bank Lending Channel: impact on credit supply and the real economy,* Journal of International Economics, v. 126, article 103328, **WP 1032 (October 2015).**

BRIPI F., D. LOSCHIAVO and D. REVELLI, *Services trade and credit frictions: evidence with matched bank – firm data,* The World Economy, v. 43, 5, pp. 1216-1252, **WP 1110 (April 2017).**

BRONZINI R., G. CARAMELLINO and S. MAGRI, *Venture capitalists at work: a Diff-in-Diff approach at late-stages of the screening process,* Journal of Business Venturing, v. 35, 3, **WP 1131 (September 2017).**

BRONZINI R., S. MOCETTI and M. MONGARDINI, *The economic effects of big events: evidence from the Great Jubilee 2000 in Rome,* Journal of Regional Science, v. 60, 4, pp. 801-822, **WP 1208 (February 2019).**

COIBION O., Y. GORODNICHENKO and T. ROPELE, *Inflation expectations and firms' decisions: new causal evidence,* Quarterly Journal of Economics, v. 135, 1, pp. 165-219, **WP 1219 (April 2019).**

CORSELLO F. and V. NISPI LANDI, *Labor market and financial shocks: a time-varying analysis,* Journal of Money, Credit and Banking, v. 52, 4, pp. 777-801, **WP 1179 (June 2018).**

COVA P. and F. NATOLI, *The risk-taking channel of international financial flows,* Journal of International Money and Finance, v. 102, **WP 1152 (December 2017).**

D'ALESSIO G., *Measurement errors in survey data and the estimation of poverty and inequality indices,* Statistica Applicata - Italian Journal of Applied Statistics, v. 32, 3, **WP 1116 (June 2017).**

DEL PRETE S. and S. FEDERICO, *Do links between banks matter for bilateral trade? Evidence from financial crises,* Review of World Economic, v. 156, 4, pp. 859 - 885, **WP 1217 (April 2019).**

D'IGNAZIO A. and C. MENON, *The causal effect of credit Guarantees for SMEs: evidence from Italy,* The Scandinavian Journal of Economics, v. 122, 1, pp. 191-218, **WP 900 (February 2013).**

ERCOLANI V. and F. NATOLI, *Forecasting US recessions: the role of economic uncertainty,* Economics Letters, v. 193, **WP 1299 (October 2020).**

MAKINEN T., L. SARNO and G. ZINNA, *Risky bank guarantees,* Journal of Financial Economics, v. 136, 2, pp. 490-522, **WP 1232 (July 2019).**

MODENA F., E. RETTORE and G. M. TANZI, *The effect of grants on university dropout rates: evidence from the Italian case,* Journal of Human Capital, v. 14, 3, pp. 343-370, **WP 1193 (September 2018).**

NISPI LANDI V., *Capital controls spillovers,* Journal of International Money and Finance, v. 109, **WP 1184 (July 2018).**

PERICOLI M., *On risk factors of the stock–bond correlation,* International Finance, v. 23, 3, pp. 392-416, **WP 1198 (November 2018).**

RAINONE E., *The network nature of OTC interest rates,* Journal of Financial Markets, v.47, article 100525, **WP 1022 (July 2015).**

RAINONE E. and F. VACIRCA, *Estimating the money market microstructure with negative and zero interest rates,* Quantitative Finance, v. 20, 2, pp. 207-234, **WP 1059 (March 2016).**

RIZZICA L., *Raising aspirations and higher education. Evidence from the UK's widening participation policy,* Journal of Labor Economics, v. 38, 1, pp. 183-214, **WP 1188 (September 2018).**

SANTIONI, R., F. SCHIANTARELLI and P. STRAHAN, *Internal capital markets in times of crisis: the benefit of group affiliation*, Review of Finance, v. 24, 4, pp. 773-811, **WP 1146 (October 2017).**

SCHIANTARELLI F., M. STACCHINI and P. STRAHAN, *Bank Quality, judicial efficiency and loan repayment delays in Italy,* Journal of Finance , v. 75, 4, pp. 2139-2178, **WP 1072 (July 2016).**

2021

ALBANESE G., E. CIANI and G. DE BLASIO, *Anything new in town? The local effects of urban regeneration policies in Italy,* Regional Science and Urban Economics, v. 86, **WP 1214 (April 2019).**

FIDORA M., C. GIORDANO and M. SCHMITZ, *Real exchange rate misalignments in the Euro Area,* Open Economies Review, v. 32, 1, pp. 71-107, **WP 1162 (January 2018).**

LI F., A. MERCATANTI, T. MAKINEN and A. SILVESTRINI, *A regression discontinuity design for ordinal running variables: evaluating central bank purchases of corporate bonds,* The Annals of Applied Statistics, v. 15, 1, pp. 304-322, **WP 1213 (March 2019).**

LOSCHIAVO D., *Household debt and income inequality: evidence from Italian survey data,* Review of Income and Wealth. v. 67, 1, pp. 61-103, **WP 1095 (January 2017).**

NISPI LANDI V. and A. SCHIAVONE, *The effectiveness of capital controls,* Open Economies Review, v. 32, 1, pp. 183-211, **WP 1200 (November 2018).**

PEREDA FERNANDEZ S., *Copula-based random effects models for clustered data,* Journal of Business & Economic Statistics, v. 39, 2, pp. 575-588, **WP 1092 (January 2017).**

FORTHCOMING

ACCETTURO A., A. LAMORGESE, S. MOCETTI and D. PELLEGRINO, *Housing Price elasticity and growth: evidence from Italian cities,* Journal of Economic Geography, **WP 1267 (March 2020).**

ALBANESE G., G. DE BLASIO and A. LOCATELLI, *Does EU regional policy promote local TFP growth? Evidence from the Italian Mezzogiorno,* Papers in Regional Science, **WP 1253 (December 2019).**

ANZUINI A. and L. ROSSI, *Fiscal policy in the US: a new measure of uncertainty and its effects on the American economy*, Empirical Economics, **WP 1197 (November 2018).**

APRIGLIANO V. and D. LIBERATI, *Using credit variables to date business cycle and to estimate the probabilities of recession in real time*, The Manchester School, **WP 1229 (July 2019).**

BALTRUNAITE A., C. GIORGIANTONIO, S. MOCETTI and T. ORLANDO, Discretion and supplier selection in public procurement, Journal of Law, Economics, and Organization, **WP 1178 (June 2018)**

COVA P., P. PAGANO, A. NOTARPIETRO and M. PISANI, *Secular stagnation, R&D, public investment and monetary policy: a global-model perspective,* Macroeconomic Dynamics, **WP 1156 (December 2017).**

DE PHILIPPIS M., *Multitask agents and incentives: the case of teaching and research for university professors,* Economic Journal, **WP 1042 (December 2015).**

DEL PRETE S. and M. L. STEFANI, *Women as "Gold Dust": gender diversity in top boards and the performance of Italian banks,* Economic Notes, Monte dei Paschi di Siena, **WP 1014 (June 2015).**

HERTWECK M., V. LEWIS and S. VILLA, *Going the extra mile: effort by workers and job-seekers,* Journal of Money, Credit and Banking, **WP 1277 (June 2020).**

METELLI L. and F. NATOLI, *The international transmission of US tax shocks: a proxy-SVAR approach,* IMF Economic Review, **WP 1223 (June 2019).**

MOCETTI S., G. ROMA and E. RUBOLINO, *Knocking on parents' doors: regulation and intergenerational mobility,* Journal of Human Resources, **WP 1182 (July 2018).**

PERICOLI M. and M. TABOGA, *Nearly exact Bayesian estimation of non-linear no-arbitrage term-structure models,* Journal of Financial Econometrics, **WP 1189 (September 2018).**